

Tomato class II glutaredoxin mutants generated via multiplex CRISPR/Cas9 genome editing technology are susceptible to multiple abiotic stresses

by

Tayebeh Kakeshpour

B.S., University of Tabriz, 2012
M.S., Tarbiat Modares University, 2015

AN ABSTRACT OF A DISSERTATION

submitted in partial fulfillment of the requirements for the degree

DOCTOR OF PHILOSOPHY

Department of Horticulture and Natural Resources
College of Agriculture

KANSAS STATE UNIVERSITY
Manhattan, Kansas

2020

ABSTRACT

Gene silencing technologies such as clustered regulatory short palindromic repeats (CRISPR)/Cas9 and RNA interference (RNAi) created a revolution in genome engineering. They are highly site-specific, simple, fast, and cost-effective. Since their discovery, gene silencing technologies have extensively been implemented in various organisms including humans, animals, plants, and microbes. They have been used for both basic science studies such as gene functional analysis and applied science such as medicine and crop improvement. In this work, we used multiplex CRISPR/Cas9 system to knock out all four members of the class II glutaredoxin (GRX) gene family including *S14*, *S15*, *S16* and *S17* in tomato and RNAi technology to express mouse complement 3 (*C3*) and complement factor 7 (*CF7*) small interfering RNAs (siRNAs) in lettuce.

Reactive oxygen species (ROS) are induced under abiotic and biotic stresses and also as byproducts of aerobic metabolism, and their overproduction causes oxidative damage to macromolecules such as proteins, lipids, carbohydrates, and nucleic acids. GRXs are small ubiquitous proteins that are known to be involved in cellular redox homeostasis by reducing disulfate bonds and scavenging ROS. To investigate the functions of each member of class II GRX gene family in tomato's response to abiotic stresses, single and multiple knockout lines for class II GRXs were obtained using multiplex CRISPR/Cas9 system. Mutant lines and wild-type plants were subjected to heat, drought, chilling, cadmium (Cd) toxicity, and short photoperiod stresses. Phenotyping data showed that members of the class II GRX gene family are critical for tomato's growth, development, and survival under several abiotic stresses. Our findings propose novel functions for members of class II *SIGRXs*.

RNAi technology can be utilized to target disease-related proteins. However, the application of siRNAs is challenging predominantly due to the difficult delivery and instability of siRNA into the host system. Recent findings of bioactivity and bioavailability of plants' miRNAs

through animals' digestive systems led to the newly introduced field of dietary siRNAs. Animal's siRNA can be expressed in plant tissues and delivered as dietary siRNA. Here, an expression vector made based on a rice miRNA backbone, Osa-MIR528, was utilized to construct two plant expression vectors containing siRNAs silencing mouse C3 and CF7 proteins. Both C3 and CF7 proteins are involved in blood clotting which could lead to cardiovascular dysfunction. Expression of both primary and mature C3 and CF7 siRNAs in lettuce was validated by semi quantitative real-time PCR and end-point PCR, respectively, and was confirmed via Sanger sequencing. Established amiRNA system in lettuce through this work will have further applications. As an edible leafy plant with high biomass, lettuce can be used as a valuable host to produce various diseases targeting siRNAs.

Tomato class II glutaredoxin mutants generated via multiplex CRISPR/Cas9 genome editing technology are susceptible to multiple abiotic stresses

by

Tayebeh Kakeshpour

B.S., University of Tabriz, 2012
M.S., Tarbiat Modares University, 2015

A DISSERTATION

submitted in partial fulfillment of the requirements for the degree

DOCTOR OF PHILOSOPHY

Department of Horticulture and Natural Resources
College of Agriculture

KANSAS STATE UNIVERSITY
Manhattan, Kansas

2020

Approved by:

Major Professor
Professor Sunghun Park

Copyright

© Tayebeh Kakeshpour 2020.

ABSTRACT

Gene silencing technologies such as clustered regulatory short palindromic repeats (CRISPR)/Cas9 and RNA interference (RNAi) created a revolution in genome engineering. They are highly site-specific, simple, fast, and cost-effective. Since their discovery, gene silencing technologies have extensively been implemented in various organisms including humans, animals, plants, and microbes. They have been used for both basic science studies such as gene functional analysis and applied science such as medicine and crop improvement. In this work, we used multiplex CRISPR/Cas9 system to knock out all four members of the class II glutaredoxin (GRX) gene family including *S14*, *S15*, *S16* and *S17* in tomato and RNAi technology to express mouse complement 3 (*C3*) and complement factor 7 (*CF7*) small interfering RNAs (siRNAs) in lettuce.

Reactive oxygen species (ROS) are induced under abiotic and biotic stresses and also as byproducts of aerobic metabolism, and their overproduction causes oxidative damage to macromolecules such as proteins, lipids, carbohydrates, and nucleic acids. GRXs are small ubiquitous proteins that are known to be involved in cellular redox homeostasis by reducing disulfate bonds and scavenging ROS. To investigate the functions of each member of class II GRX gene family in tomato's response to abiotic stresses, single and multiple knockout lines for class II GRXs were obtained using multiplex CRISPR/Cas9 system. Mutant lines and wild-type plants were subjected to heat, drought, chilling, cadmium (Cd) toxicity, and short photoperiod stresses. Phenotyping data showed that members of the class II GRX gene family are critical for tomato's growth, development, and survival under several abiotic stresses. Our findings propose novel functions for members of class II *SIGRXs*.

RNAi technology can be utilized to target disease-related proteins. However, the application of siRNAs is challenging predominantly due to the difficult delivery and instability of siRNA into the host system. Recent findings of bioactivity and bioavailability of plants' miRNAs

through animals' digestive systems led to the newly introduced field of dietary siRNAs. Animal's siRNA can be expressed in plant tissues and delivered as dietary siRNA. Here, an expression vector made based on a rice miRNA backbone, Osa-MIR528, was utilized to construct two plant expression vectors containing siRNAs silencing mouse C3 and CF7 proteins. Both C3 and CF7 proteins are involved in blood clotting which could lead to cardiovascular dysfunction. Expression of both primary and mature C3 and CF7 siRNAs in lettuce was validated by semi quantitative real-time PCR and end-point PCR, respectively, and was confirmed via Sanger sequencing. Established amiRNA system in lettuce through this work will have further applications. As an edible leafy plant with high biomass, lettuce can be used as a valuable host to produce various diseases targeting siRNAs.

Table of Contents

List of Figures	x
List of Tables	xi
Acknowledgements	xii
Dedication	xiv
Chapter 1 - Introduction	1
RNAi	1
ZFNs and TALENs	2
CRISPR/Cas9	3
History	3
Mechanism	4
Applications	5
Regulation	6
REFERENCES	8
Chapter 2 - Tomato class II glutaredoxin mutants generated via multiplex CRISPR/Cas9 genome editing technology are susceptible to multiple abiotic stresses	13
ABSTRACT	13
INTRODUCTION	14
MATERIALS AND METHODS	18
Selection of target sequences and vector construction	18
Plant transformation	18
DNA isolation, transgenic screening and genotyping	19
Heat stress assay	20
Drought stress assay	20
Chilling stress assay	21
Cadmium toxicity assay	21
Photoperiod and nutrient assays	22
Growth chamber experiments	22
Greenhouse experiments	22
RESULTS	24
Characterization of CRISPR/Cas9 targeted mutations in T0 transgenic plants	24
Inheritance and stability of targeted mutations in T1 and T2 mutant lines	25
<i>Slgrx</i> null mutants have reduced heat tolerance	27
<i>Slgrx</i> null mutants have reduced drought resistance	27
<i>Slgrx</i> null mutants have reduced chilling tolerance	28
<i>Slgrx</i> null mutants have reduced growth under cadmium toxicity	28
<i>Slgrx</i> null mutants have reduced growth and delayed flowering under short photoperiod... ..	29
Growth chamber experiments	29
Greenhouse experiments	29
DISCUSSIONS	32
Heat stress	33
Drought stress	35
Chilling stress	35
Cadmium toxicity	36
Photoperiod	38

CONCLUSIONS	40
REFERENCES	42
FIGURES	50
TABLES	66
SUPPLEMENTARY FIGURES.....	73
Chapter 3 - Expression of mouse small interfering RNAs in lettuce using artificial microRNA technology.....	74
ABSTRACT.....	74
INTRODUCTION	75
MATERIALS AND METHODS.....	78
Plasmid construction	78
Plant material, transformation and growth condition.....	78
DNA isolation and screening for putatively transformed plants.....	79
Quantitative real-time PCR analysis for absolute quantification of transgene copy number	79
RNA isolation, semi-quantitative RT-PCR and end-point PCR analysis	80
Quantitative real-time PCR analysis	81
RESULTS	83
Construction of siRNA expression vectors	83
Analysis of transgenic plants by PCR.....	83
Detection of primary and mature siRNAs.....	84
Relative expression levels of mature amiRNAs	84
DISCUSSION.....	86
REFERENCES	87
FIGURES	93
TABLES	99

List of Figures

Figure 2-1 CRISPR/Cas9 binary vector harboring guide RNA array designed to target <i>S14</i> , <i>S15</i> , <i>S16</i> and <i>S17</i> glutaredoxins in tomato.	50
Figure 2-2 Genotyping analysis of CRISPR/Cas9-induced mutations in T0 transgenic tomato plants.	52
Figure 2-3 Phenotypic analysis of <i>s14</i> , <i>s16</i> , <i>s17</i> single, <i>s14::16</i> double, and <i>s14::16::17</i> triple mutant tomato lines in response to heat stress.	53
Figure 2-4 Phenotypic analysis of <i>s14</i> , <i>s16</i> , <i>s17</i> single, <i>s14::16</i> double and <i>s14::16::17</i> triple mutant tomato lines in response to drought stress.	54
Figure 2-5 Phenotypic analysis of <i>s14</i> , <i>s16</i> , <i>s17</i> single, <i>s14::16</i> double, and <i>s14::16::17</i> triple mutant tomato lines in response to chilling stress.	55
Figure 2-6 Phenotypic analysis of <i>s14</i> , <i>s16</i> , <i>s17</i> single, <i>s14::16</i> double, and <i>s14::16::17</i> triple mutant tomato lines in response to cadmium toxicity stress.	57
Figure 2-7 Phenotypic analysis of wild-type and mutant lines under different photoperiods in growth chambers.	59
Figure 2-8 Phenotypic analysis of wild-type and mutant tomato lines under different levels of nutrients and photoperiods in greenhouse.	60
Figure 2-9 Shoot fresh weight of wild-type and mutant tomato lines under different levels of nutrients and photoperiods.	61
Figure 2-10 Flowering time of wild-type and mutant tomato lines under different levels of nutrients and photoperiods.	65
Figure 3-1 Plant expression vectors harboring amiRNAs designed to target C3 and CF7 messenger RNAs of mouse using a 245-bp fragment of <i>osa-MIR528</i>	93
Figure 3-2 Molecular and phenotype analyses of C3siRNA- and CF7siRNA-expressing lettuces.	94
Figure 3-3 Absolute quantification of transgene copy number in <i>C3siRNA</i> - and <i>CF7siRNA</i> -expressing lettuces using quantitative real-time PCR.	95
Figure 3-4 PCR detection of primary and mature amiRNAs and Sanger sequencing of mature C3 and CF7 amiRNAs using stem-loop universal reverse primer.	96
Figure 3-5 Quantitative real-time PCR analysis of mature C3 and CF7 artificial microRNAs (amiRNAs) in <i>C3siRNA</i> - and <i>CF7siRNA</i> -expressing lettuces using stem-loop primer.	97

List of Tables

Table 2-1 List of primers used for screening and genotyping CRISPR/Cas9 generated class II <i>Slgrxs</i> mutant lines.....	66
Table 2-2 T0 transgenic tomato lines generated using the CRISPR/Cas9 system.	67
Table 2-3 Guide RNA efficiency in Agrobacterium-mediated gene transformation of tomato. ..	67
Table 2-4 Detected genotype of T1 Transgenic tomato lines segregated from CRISPR/Cas9 generated T0 parents.	68
Table 2-5 Detected genotype of T2 transgenic tomato lines segregated from T1 CRISPR/Cas9 mutated lines.	69
Table 2-6 Three-way ANOVA for shoot fresh weight in wild-type and <i>s14</i> , <i>s16</i> , <i>s17</i> , <i>s14::16</i> , and <i>s14::16::17</i> mutant lines.	70
Table 2-7 Three-way ANOVA for flowering time in wild-type and <i>s14</i> , <i>s16</i> , <i>s17</i> , <i>s14::16</i> and <i>s14::16::17</i> mutant lines.	71
Table 2-8 Summary of phenotyping analysis in wild-type and <i>s14</i> , <i>s16</i> , <i>s17</i> , <i>s14::16</i> and <i>s14::16::17</i> mutant lines.	72
Table 3-1 Primer sequences.....	99

Acknowledgements

I would like to thank everyone who supported me during my doctoral study in Kansas State University and Horticulture and Natural Resources Department.

I am forever grateful to my advisor, Dr. Sunghun Park for all he has done for me. Joining his lab was the best thing happened in my career, and without his support I would not be where I am today. He sincerely and generously advised me throughout every step of my research. I admire him for his respect and kindness for students and if I am to be an academic advisor one day, he is my role model; He taught me how to be an excellent teacher by example.

I would like to thank my committee members for their guidance and support during my Ph.D. training. Dr. Dale Bremer who taught me importance of nicely presenting data as a scientist and how to be a confident speaker by a simple sentence “If you are here to speak, you earned it!”. I remind this to myself before any presentation and takes away my anxiety! Dr. C.B. Rajashekar who I truly enjoyed his classes where I broadened my knowledge on abiotic stresses physiology. Dr. Mithila Jugulam who taught me to look at my research and its applications from a different perspective. Dr. Mark Ungerer for his valuable advice and suggestions on my dissertation and defense.

I would like to thank my lab members who made a second home for me. My sincere thanks to Kim Park for the valuable transgenic research materials she provided for me, and mentally supporting me when I needed it the most. Many thanks to Tej Man Tamang for always being there for me with his sensible critiques, comments and suggestions on my research, and helping me in conducting research. Spencer Navrude, Gergely Motolai, and Zachary Fleming are kind and supportive lab mates and always helped me in greenhouse and lab when I needed their help. Our former graduate students Dr. Qingyu Wu, Dr. Stuart Sprague, and Dr. Ying Hu who constantly

shared their invaluable knowledge and experiences with me. Dan Park for providing me valuable transgenic materials that made this research possible.

I would like to thank our collaborator Dr. Hirschi Kendal and his research group Dr. Murli Manohar and Dr. Jian Yang for their assistance in lettuce work.

I would like to thank all faculty, staff and students in our Horticulture and Natural Resources family who made my Ph.D. experience more enjoyable with providing friendly atmosphere. My amazing friends Tej Man Tamang, Myungjin Lee, and Anuja Paudyal who helped me get through hardest days.

My parents Masoomah and Dariush have given me everything they had even their simplest parental right to visit their child. My older brother, Tayeb is my first teacher and taught me how to dream, dedicate and succeed. My younger brother, Ali is my happiness. My best friend Kumar gave me a second family. Thank you all, I could not have asked for more in my life.

Dedication

I dedicate this work to all the nurses and doctors who lost or risked their lives saving us from Covid-19 pandemic. If it was not for their constant sacrifices, I may not have been able to finish this dissertation. May you be safe.

Chapter 1 - Introduction

Genome editing and gene silencing are technologies that enable manipulation of the DNA and RNA in living organisms. Unlike, previous genetic engineering techniques, that create random DNA modifications such as insertions or deletions, gene silencing technologies such as RNA interference (RNAi), zinc-finger nucleases (ZFNs), transcription activator-like effector nucleases (TALENs), and clustered regulatory interspaced short palindromic repeats (CRISPR)/Cas9 are highly site-specific. In 2011, ZFNs and TALENs were selected as methods of the year by Nature Methods, and in 2015 CRISPR/Cas9 was selected as a breakthrough of the year by Science. Genome engineering tools are used in basic and applied sciences. In this dissertation, we implemented CRISPR/Cas9 and RNAi technologies for targeted gene silencing in crops aimed at gene functional analysis and therapeutic purposes.

RNAi

RNAi mechanism is a natural process that can introduce sequence-specific messenger RNA (mRNA) and protein knockdown through small interference RNAs (siRNAs) and microRNAs (miRNAs). RNAi knocks down gene expression in three different levels by inhibiting DNA transcription, mRNA intermediates, or translation (Novina et al., 2004). In 1998, the RNAi process was discovered by Andrew Fire and Craig C. Mello and in 2006 the two scientists won Noble Prize in physiology and medicine for RNAi discovery (Fire & Mello, 2006). RNAi is an ancient genome defense mechanism that inhibits invading genetic materials such as transposons and viruses, also involved in gene regulation and divergence (Schramke & Allshire, 2003).

siRNA is a short, 20-25 nucleotide, non-coding double-stranded RNA (dsRNA) which is catalyzed by an endo-ribonuclease enzyme called Dicer (Bernstein et al., 2001). Like siRNA, miRNA is also a small, 22 nucleotide non-coding RNA that functions in the RNAi process, but

unlike siRNA, miRNA is not generated from dsRNA. Instead, miRNA is generated when single-stranded endogenous RNA or primary RNA (pri-miRNA) which is transcribed by RNA polymerase II, folds back, its complementary regions bind and create a small hairpin structure. Primary miRNA (Pri-miRNA) is cleaved by an enzyme called DROSHA to form precursor miRNA (pre-miRNA). Dicer cleaves long, dsRNA to form short dsRNA. Short siRNA/miRNA will then bind to other proteins to form the RNA-Induced Silencing Complex (RISC). After attaching to RISC, dsRNA denatures and forms single-stranded RNA. One of the strands (sense or passenger) is degraded and the other strand (anti-sense or guide) which is the less stable strand and is complementary to target mRNA remains attached to the RISC. Guide strand directs RISC to the complementary mRNA where cleavage is induced by an enzyme called Argonaute (AGO). As a result, the targeted mRNA will not produce any proteins, and the gene is silenced. siRNAs are a hundred percent complementary to their target mRNAs, while miRNAs do not need perfect base-pairing with their target, so they can target multiple mRNAs and compare to siRNAs are less specific (Baulcombe, 2004; Manjunath et al., 2010). Exogenously introduced siRNAs can be used to knock down any target gene, hence RNAi technology has had a great impact on functional analysis of genes without the use of other complicated technologies.

ZFNs and TALENs

ZFNs and TALENs are DNA-binding molecules that contain two components, a DNA-binding domain that can be designed to target any sequence, and a cleavage domain. DNA-binding domain of ZFNs contains three to six zinc-finger repeats, recognizing 9 to 18 bp with each zinc-finger repeat being able to recognize 3 bp. Thus, an array of 3 zinc-fingers can be designed to target a 9 bp specific DNA site (Ramirez et al., 2008). DNA-binding domain of TALENs contains repeated 33-34 amino acids which are highly conserved. Amino acids 12th and 13th are on the other hand

highly variable and can recognize specific nucleotides. These two positions can be engineered to make specific DNA-binding domains using different amino acid combinations that can recognize the target DNA site (Boch et al., 2009; Moscou & Bogdanove 2009). Cleavage domain of ZFNs and TALENs are a restriction endonuclease FokI which is a bacterial type II endonuclease. FokI has an N-terminal DNA-binding domain that binds to double-stranded DNA and creates a non-specific double-stranded break (DSB) at C-terminal (Kim et al., 1996). ZFNs are used for disabling alleles, allele editing, and gene therapy (Durai et al., 2005). TALENs are used to improve food crops, biofuel production, resistance to diseases by creating genome modifications through gene knock out and knock-in (Daboussi et al., 2014; de León et al., 2014; Haun et al., 2014; Wienert et al., 2015). Possibility of off-target cleavage is the main drawback of ZFNs and TALENs if they do not target a unique site or have enough specificity to their target sites. Moreover, utilizing ZFNs and TALENs are costly, less efficient, and time-consuming.

CRISPR/Cas9

ZFNs and TALENs have been helpful for basic and applied biological studies, but they are costly, laborious, and inefficient. However, emerging of the CRISPR/Cas9 system solved the above-mentioned problems of previous genome editing technologies. Moreover, CRISPR/Cas9 system has infrequent off-target mutations and high mutation efficiency (Zhou et al., 2014; Bortesi et al., 2015; Li et al., 2018; Li et al., 2018).

History

In 1987, Yoshizumi Ishino and his colleagues at Osaka University accidentally cloned clustered DNA repeats along with their target gene. They noticed the unusual clustered repeats, however at the time they did not know their function (Ishino et al., 1987). Later in 1993, the interrupted clustered repeats were found in *Mycobacterium tuberculosis* by researchers in Netherland. They

observed that DNA sequences in-between the repeated clusters varied in different strains of the bacterium (Van Soolingen et al., 1993). About the same time at the University of Alicante in Spain Francisco Mojica found clustered repeats in two species, *Haloferax* and *Haloarcula*. He tried to study their functions and suggested that they are involved in cell division, however, his hypothesis was wrong. In 2001, his student and Mojica found these clusters of interrupted repeats in 20 more microbe species and named them CRISPR (Mojica et al., 2000; Mojica & Montoliu 2016; Mojica & Rodriguez-Valera 2016). A year later CRISPR sequences were reported to be transcribed into RNA (Charpentier et al., 2015). In 2002, also several genes encoding enzymes with helicase and nuclease activities were found near CRISPR regions. These enzymes were named CRISPR associated systems or Cas proteins (Jansen et al., 2002). Finally, in 2005, three independent groups found that the spacer DNA between the clustered repeats is the DNA from bacteriophages and viruses suggesting their function in adaptive immunity against viruses and bacteriophages (Bolotin et al., 2005; Mojica et al., 2005; Pourcel et al., 2005). CRISPR is a four-component system including a Cas protein such as Cas9 or Cas12a, trans-activating CRISPR RNA or tracrRNA, and two small CRISPR RNAs (crRNA). In an incredible work, Jennifer Doudna and Emmanuelle Charpentier simplified CRISPR/Cas9 system in *Streptococcus pyogenes* into a two-component system including Cas9 protein and guide RNA (gRNA) which is made of tracrRNA and crRNA combined (Jinek et al., 2012).

Mechanism

In this system, Cas9 endonuclease is coupled with a chimeric single guide RNA (sgRNA) to form a nuclease-based genome editing tool (Kabadi et al., 2014). The first 20 nucleotides of sgRNA are complementary to the desired DNA target and recognize 5'-NGG or protospacer adjutant motif (PAM) sequence and guide Cas9 to induce double-strand breaks (DSBs) 3-4 bp upstream of the

PAM (Li et al., 2018). DSBs are repaired by homologous recombination (HR) or homology-directed repair (HDR) and non-homologous end joining (NHEJ). Via utilizing HDR an exogenous DNA sequence can be knocked into the genome through DNA break and repair by using a specific DNA sequence as a repair template. NHEJ is an error-prone mechanism that creates insertions and deletions at target sequence, causing loss of gene function, thus it is used for gene knock out (Li et al., 2018; Yu et al., 2017).

Applications

Because of its sequence-specific editing, CRISPR/Cas9 technology can be used to repair disease-causing mutations, thus has the potential to treat various human diseases, especially those which are originated from a genetic disorder such as cancer, sickle cell anemia, hemophilia, cystic fibrosis and Huntington's disease (Cai et al., 2016). Since 2016 CRISPR based clinical trials for cancer treatment were approved by FDA and since then it has been on a clinical trial to edit mutations in genes causing cancer by several different research groups (Cyranoski 2016; Khan et al., 2016). CRISPR can be implemented for antimicrobial therapy; A more aggressive type of CRISPR system, CRISPR/Cas3, can be used to target invading viruses or manipulation of the CRISPR region of bacteria can control their population (Cai et al., 2016; Goma et al., 2014). CRISPR interfering (CRISPRi) system containing unfunctional or dead Cas9 (dCas9) which lacks nuclease activity is another application of the CRISPR system. It is similar to RNAi except that RNAi targets mRNA while CRISPRi targets DNA at the transcription level and inhibits RNA polymerase from binding to promoter causing sequence-specific gene silencing without creating DNA breakage (Dominguez et al., 2016). CRISPR activation (CRISPRa) is another application of CRISPR that utilizes Cas9 to carry transcription enhancers for a certain target gene and increase its expression level (Pennisi, 2013). Not only CRISPR system can target and break DNA

molecules, but it was discovered that the CRISPR system in some bacteria can recognize and break RNA from invading viruses thus making it a tool for editing RNA molecules (Zimmer, 2016). CRISPR/Cas9 system can be precisely designed to generate multiplex genome editing by targeting multiple target sites simultaneously using a single Cas9 construct containing more than one sgRNA, hence providing a powerful tool for generating multiple mutants containing edits in different genes (Bortesi et al., 2015). The later application of CRISPR/Cas9 makes it a unique system to study gene families much more efficient than previous methods. To create double mutants, single mutants are crossed and progeny are screened for double mutants, and it gets more difficult and higher numbers of crosses and generations to be screened are required which might take up to years when a triple, quadruple or higher number of genes are required to be knocked out in a single plant. However, the CRISPR/Cas9 system can theoretically target any numbers of genes in one single generation and speed up functional genome studies.

Regulation

CRISPR/cas9 edited crops are not regulated by food and drug administration (FDA). In such a short time after the emergence of CRISPR as an editing tool in plants, many crops edited by CRISPR with improved economical and agronomical features are already under research, trial or approved by the US department of agriculture (USDA) and awaiting FDA approval. In cotton CRISPR/Cas9 was applied to produce cotton seeds that do not contain gossypol thus can be used as food (Folta, 2019). Tomatoes are an example of the successful implication of CRISPR in many current studies. In one research by Zsögön et al. (2016), CRISPR is used to create tomatoes with higher nutrient content, higher yield and higher abiotic stress tolerance. In mushroom, CRISPR knock out of one polyphenol oxidase gene by Yinong Yang resulted in reduced browning by 30%. Miao et al., used CRISPR to knock out a series of rice genes that resulted in increased grain yield

by 25-31%. Disruption of *TcNPR3* in cocoa using CRISPR done by Fister et al., increased Cocoa's resistance against *Phytophthora tropicalis*. Sánchez-Léon et al., used CRISPR to successfully mutate 34 gluten production genes resulted in low gluten content wheat which caused up to 85% reduction in immunoreactivity. In citrus CRISPR was used by Nian Wang to edit oranges against citrus greening disease (<https://www.synthego.com/blog/crispr-agriculture-foods#crops>).

REFERENCES

- Baulcombe, D. (2004). RNA silencing in plants. *Nature*, *431*(7006), 356-363.
- Bernstein, E., Caudy, A. A., Hammond, S. M., & Hannon, G. J. (2001). Role for a bidentate ribonuclease in the initiation step of RNA interference. *Nature*, *409*(6818), 363-366.
- Boch, J., Scholze, H., Schornack, S., Landgraf, A., Hahn, S., Kay, S., & Bonas, U. (2009). Breaking the code of DNA binding specificity of TAL-type III effectors. *Science*, *326*, 1509-1512.
- Bolotin, A., Quinquis, B., Sorokin, A., & Ehrlich, S. D. (2005). Clustered regularly interspaced short palindrome repeats (CRISPRs) have spacers of extrachromosomal origin. *Microbiology*, *151*, 2551-2561.
- Bortesi, L., & Fischer, R. (2015). The CRISPR/Cas9 system for plant genome editing and beyond. *Biotechnology advances*, *33*, 41-52.
- Cai, L., Fisher, A. L., Huang, H., & Xie, Z. (2016). CRISPR-mediated genome editing and human diseases. *Genes & diseases*, *3*(4), 244-251.
- Charpentier, E., Richter, H., van der Oost, J., & White, M. F. (2015). Biogenesis pathways of RNA guides in archaeal and bacterial CRISPR-Cas adaptive immunity. *FEMS microbiology reviews*, *39*(3), 428-441.
- Cyranoski, D. (2016). CRISPR gene-editing tested in a person for the first time. *Nature news*, *539*(7630), 479.
- Daboussi, F., Leduc, S., Maréchal, A., Dubois, G., Guyot, V., Perez-Michaut, C., ... & Voytas, D. F. (2014). Genome engineering empowers the diatom *Phaeodactylum tricornutum* for biotechnology. *Nature communications*, *5*(1), 1-7.

- de León, V. P., Merillat, A. M., Tesson, L., Anegón, I., & Hummler, E. (2014). Generation of TALEN-mediated GRdim knock-in rats by homologous recombination. *PLoS One*, *9*(2).
- Dominguez, A. A., Lim, W. A., & Qi, L. S. (2016). Beyond editing: repurposing CRISPR–Cas9 for precision genome regulation and interrogation. *Nature reviews Molecular cell biology*, *17*(1), 5.
- Durai, S., Mani, M., Kandavelou, K., Wu, J., Porteus, M. H., & Chandrasegaran, S. (2005). Zinc finger nucleases: custom-designed molecular scissors for genome engineering of plant and mammalian cells. *Nucleic acids research*, *33*(18), 5978-5990.
- Fire, A. Z., & Mello, C. C. (2006). The Nobel prize in physiology or medicine 2006. Nobel Media AB 2014.
- Gomaa, A. A., Klumpe, H. E., Luo, M. L., Selle, K., Barrangou, R., & Beisel, C. L. (2014). Programmable removal of bacterial strains by use of genome-targeting CRISPR-Cas systems. *MBio*, *5*(1), e00928-13.
- Haun, W., Coffman, A., Clasen, B. M., Demorest, Z. L., Lowy, A., Ray, E., ... & Mathis, L. (2014). Improved soybean oil quality by targeted mutagenesis of the fatty acid desaturase 2 gene family. *Plant biotechnology journal*, *12*(7), 934-940.
- Ishino, Y., Shinagawa, H., Makino, K., Amemura, M., & Nakata, A. (1987). Nucleotide sequence of the *iap* gene, responsible for alkaline phosphatase isozyme conversion in *Escherichia coli*, and identification of the gene product. *Journal of bacteriology*, *169*(12), 5429-5433.
- Jansen, R., Embden, J. D. V., Gaastra, W., & Schouls, L. M. (2002). Identification of genes that are associated with DNA repeats in prokaryotes. *Molecular microbiology*, *43*(6), 1565-1575.

- Jinek, M., Chylinski, K., Fonfara, I., Hauer, M., Doudna, J. A., & Charpentier, E. (2012). A programmable dual-RNA-guided DNA endonuclease in adaptive bacterial immunity. *science*, 337(6096), 816-821.
- Kabadi, A. M., Ousterout, D. G., Hilton, I. B., & Gersbach, C. A. (2014). Multiplex CRISPR/Cas9-based genome engineering from a single lentiviral vector. *Nucleic acids research*, 42(19), e147-e147.
- Kevin F., *Ancestry & Evolution*, 2019.
- Khan, F. A., Pandupuspitasari, N. S., Chun-Jie, H., Ao, Z., Jamal, M., Zohaib, A., ... & ShuJun, Z. (2016). CRISPR/Cas9 therapeutics: a cure for cancer and other genetic diseases. *Oncotarget*, 7(32), 52541.
- Kim, Y. G., Cha, J., & Chandrasegaran, S. (1996). Hybrid restriction enzymes: zinc finger fusions to Fok I cleavage domain. *Proceedings of the National Academy of Sciences*, 93(3), 1156-1160.
- Li, R., Li, R., Li, X., Fu, D., Zhu, B., Tian, H., ... & Zhu, H. (2018). Multiplexed CRISPR/Cas9-mediated metabolic engineering of γ -aminobutyric acid levels in *Solanum lycopersicum*. *Plant biotechnology journal*, 16(2), 415-427.
- Li, X., Wang, Y., Chen, S., Tian, H., Fu, D., Zhu, B., ... & Zhu, H. (2018). Lycopene is enriched in tomato fruit by CRISPR/Cas9-mediated multiplex genome editing. *Frontiers in plant science*, 9, 559.
- Manjunath, N., Dykxhoorn, D. M. (2010). Advances in synthetic siRNA delivery. *Discovery medicine*, 9,418-430.

- Mojica, F. J., & Montoliu, L. (2016). On the origin of CRISPR-Cas technology: from prokaryotes to mammals. *Trends in microbiology*, 24(10), 811-820.
- Mojica, F. J., & Rodriguez-Valera, F. (2016). The discovery of CRISPR in archaea and bacteria. *The FEBS journal*, 283(17), 3162-3169.
- Mojica, F. J., Díez-Villaseñor, C., Soria, E., & Juez, G. (2000). Biological significance of a family of regularly spaced repeats in the genomes of Archaea, Bacteria and mitochondria. *Molecular microbiology*, 36(1), 244-246.
- Mojica, F. J., García-Martínez, J., & Soria, E. (2005). Intervening sequences of regularly spaced prokaryotic repeats derive from foreign genetic elements. *Journal of molecular evolution*, 60(2), 174-182.
- Moscou, M. J., & Bogdanove, A. J. (2009). A simple cipher governs DNA recognition by TAL effectors. *Science*, 326(5959), 1501-1501.
- Novina, C. D., & Sharp, P. A. (2004). *The RNAi revolution*. *Nature*, 430(6996), 161.
- Pennisi E (August 2013). "The CRISPR craze". News Focus. *Science*. 341(6148), 833-6.
- Pilon, M., Cohu, C. M., Ravet, K., Abdel-Ghany, S. E., & Gaymard, F. (2009). Essential transition metal homeostasis in plants. *Current opinion in plant biology*, 12(3), 347-357.
- Pourcel, C., Salvignol, G., & Vergnaud, G. (2005). CRISPR elements in *Yersinia pestis* acquire new repeats by preferential uptake of bacteriophage DNA and provide additional tools for evolutionary studies. *Microbiology*, 151(3), 653-663.
- Ramirez, C. L., Foley, J. E., Wright, D. A., Müller-Lerch, F., Rahman, S. H., Cornu, T. I., ... & Cathomen, T. (2008). Unexpected failure rates for modular assembly of engineered zinc fingers. *Nature methods*, 5(5), 374-375.

- Schramke, V., & Allshire, R. (2003). Hairpin RNAs and retrotransposon LTRs effect RNAi and chromatin-based gene silencing. *Science*, *301*(5636), 1069-1074.
- Van Soolingen, D., De Haas, P. E., Hermans, P. W., Groenen, P. M., & Van Embden, J. D. (1993). Comparison of various repetitive DNA elements as genetic markers for strain differentiation and epidemiology of *Mycobacterium tuberculosis*. *Journal of clinical microbiology*, *31*(8), 1987-1995.
- Wienert, B., Funnell, A. P., Norton, L. J., Pearson, R. C., Wilkinson-White, L. E., Lester, K., ... & Crossley, M. (2015). Editing the genome to introduce a beneficial naturally occurring mutation associated with increased fetal globin. *Nature communications*, *6*, 7085.
- Yu, Q. H., Wang, B., Li, N., Tang, Y., Yang, S., Yang, T., ... & Asmutola, P. (2017). CRISPR/Cas9-induced targeted mutagenesis and gene replacement to generate long-shelf life tomato lines. *Scientific reports*, *7*(1), 1-9.
- Zhou, H., Liu, B., Weeks, D. P., Spalding, M. H., & Yang, B. (2014). Large chromosomal deletions and heritable small genetic changes induced by CRISPR/Cas9 in rice. *Nucleic acids research*, *42*(17), 10903-10914.
- Zimmer, C. (2016). Scientists Find Form of Crispr Gene Editing with New Capabilities. *The New York Times*.

Chapter 2 - Tomato class II glutaredoxin mutants generated via multiplex CRISPR/Cas9 genome editing technology are susceptible to multiple abiotic stresses

ABSTRACT

Bacterial clustered regularly interspaced short palindromic repeats (CRISPR)/Cas9 system can be precisely designed to generate multiplex genome editing (multiple genes and multiple sites in a single plant), providing a powerful tool for studying functions of gene families in plants. Here, we report the targeted mutagenesis of *Solanum lycopersicum* class II glutaredoxins (*SIGRXs*) (*SIGRXS14*, *SIGRXS15*, *SIGRXS16*, and *SIGRXS17*), using a multiplex CRISPR/Cas9 system. GRXs have been reported to be involved in iron-sulfur assembly and oxidative stress responses; However, their function in plants has not been understood despite their importance. We generated various simultaneous single and multiple *SIGRX* mutant lines (*Slgrx*) in tomato using the binary pYLCRISPR/Cas9P35S-N vector. T0, T1, and T2 tomato generations were genotyped to screen for stable T-DNA free homozygous lines. Single, double, and triple homozygous *Slgrx* mutant lines for *S14*, *S16*, and *S17* GRXs were obtained and subjected to phenotypic analyses under heat, drought, chilling, heavy metal toxicity, and short photoperiod stresses. Due to embryonic lethality no homozygous mutants were obtained for *GRXS15* and phenotypic analysis were performed with five mutant lines containing mutations in three genes including *S14*, *S16*, and *S17*. Compared to wild-type, *Slgrxs* mutant lines showed higher sensitivity to several abiotic stresses. These findings suggest that class II *SIGRXs* have specific roles against abiotic stress conditions and are ideal candidates for genome engineering to improve crop tolerance to abiotic stresses.

INTRODUCTION

Recent drastic environmental changes such as massive rainfalls, floods, and drought, severe high and low temperatures, seasonal variation, forest fires, heavy metals toxicity and epidemy of new plant diseases are threads to agriculture production and food security for world's growing population (Yadav et al., 2011). It is estimated that by the year 2050 world's population will reach 9.1 billion which means there will be a need for food production to increase almost 100% to sufficiently feed the world's population (Smil, 2005; Charles et al., 2010). Climate change has been occurring due to natural climate variations or human activities such as burning fossils or converting forests to farms which emit greenhouse gases such as CO₂ and O₃. The increased concentration of greenhouse gases is the main cause of global warming, and subsequent drought and increased sea level. Increased CO₂ concentrations improve the yield of C3 plants, however, increased O₃ concentrations reduce crop yield (Burney & Ramanathan, 2014). Continued global warming will expand arid and semi-arid areas where drought can severely drop crop yield. Thus, countries located in such areas that are among the poorest countries and are already suffering from unstable food production and malnutrition due to various reasons such as urbanization and inadequate infrastructures (Hussain and Lunven, 1987), will face the highest degree of restrictions in agriculture. Additionally, being the main source of food, agriculture is also a source of income for both rural and urban populations. Hence, creating solutions to successfully face climate change and improving agricultural productivity is urgent. Cultural practices, mechanization, integrated pest management, sustainable agriculture, and genetic diversity and traditional breeding can all contribute to adapting to abiotic stresses caused by climate change (Tester & Langridge, 2010; Yadav et al., 2019), however, the mentioned solutions are not enough and have their limitations. Molecular breeding and reverse genetics via recently developed genome editing technologies such

as CRISPR/Cas9 system have great potentials to manipulate genes in agronomically important crops to enhance their quality and quantity under abiotic stress conditions. In response to unfavorable environmental conditions including heat, drought, cold and heavy metals, plants overproduce reactive oxygen species (ROS) such as $O_2^{\bullet-}$, H_2O_2 , $HO_2^{\bullet-}$, OH^{\bullet} and ROOH which are toxic, leading to unbalanced cellular homeostasis and causing oxidative damage to macromolecules such as proteins, lipids, carbohydrates and DNA (Grag et al., 2010; Li et al., 2014; Rouhier et al., 2010; Ströher et al., 2016). ROS are also produced under biotic stress conditions and as byproducts of aerobic metabolism. Overproduction of ROS under abiotic stress conditions is an important cause of yield reduction in crops while ROS are actively produced by plants and involved in signal transduction pathways to regulate several physiological mechanisms under stress condition (Mittler, 2002; Mahajan et al., 2005; Khan et al., 2008). Thus, ROS can cause damage or can act as a signaling molecule to protect plant cells depending on its concentration and production site and time, maintaining ROS homeostasis is very important. Different antioxidant systems including various enzymes such as catalase, superoxide dismutase, ascorbate peroxidase, and glutathione reductase, and molecules such as ascorbic acid, phenolic compounds, and glutathione (GSH) can scavenge ROS (Foyer and Noctor, 2005; Mittler, 2004). Plant glutaredoxins (GRXs) are a component of the antioxidant network. GRXs are 20-60 KDa ubiquitous proteins, belong to thioredoxin (TRX) superfamily with a $\beta 1-\alpha 1-\beta 2-\alpha 2-\beta 3-\beta 4-\alpha 3$ TRX fold (Garg et al., 2010; Li et al., 2014). Based on the active site motif GRXs fall into three major classes, CPYC-type, CGFS-type, and CC-type (Li et al., 2014; Rouhier et al., 2010). Class II GRXs are divided into two groups: proteins with one GRX domain such as *GRXS14*, *GRXS15*, and *GRXS16*, and proteins with one TRX domain and one, two, or three GRX domains such as *GRXS17* which has three GRX domains (Rouhier et al., 2010). CGFS-type GRXs act as scaffold proteins

for assembling [2Fe-2S] clusters, in different cellular compartments where they are localized. *GRXS14* and *GRXS16* contribute to the iron-sulfur assembly in the chloroplast (Balk and Pilon, 2011), *GRXS15* in mitochondria (Ströher et al., 2016) and *GRXS17* in the cytosol (Iñigo et al., 2016). The GRXs are also involved in oxidative stress signaling as thiol-disulfide oxidoreductases and use glutathione (GSH) as an electron donor (Rouhier et al., 2010). GRXs can post-translationally affect protein functions by reducing protein mixed disulfides through monothiol and dithiol mechanisms based on their active site, thus repairing oxidative damage of oxidized proteins or lipid hydroperoxides (Dos Santos & Rey 2006). Class II GRXs function through the monothiol mechanism, because they contain one cysteine residue in their active site (Iñigo et al., 2016). Although several studies on model plants and yeast have proposed certain important functions for the class II GRX family, the underlying mechanisms of how do class II GRXs coordinate with each other to regulate crop development under abiotic stresses remain elusive, partially due to the functional redundancy (Wu et al., 2017).

Because of their importance for plants' response to abiotic stresses as oxidoreductases, here, functions of class II GRXs were investigated. Multiplex CRISPR/Cas9 genome editing technology was implemented to mutate class II GRX gene family in tomato. In addition to its available whole genome sequence, fleshy fruit that cannot be studied in other model plants makes tomato a unique model to study plant genetics, metabolomics, and physiology of fleshy fruits (Tomato Genome Consortium, 2012). The economic importance and production increase from 27.6 million tons in 1961 to 171 million tons in 2014 which makes tomato the second most important vegetable grown worldwide explains the importance of genome functional studies in tomato (FAO, 2017). Different single, double, and triple mutant class II GRX tomato lines were exposed to different photoperiods and multiple environmental stresses including heat, drought,

chilling, and Cd toxicity to propose a possible function for each gene and their interactions under different environmental conditions.

Considering the importance of the class II GRX for plants' redox regulation, we hypothesized that due to reduced antioxidant activities and increased levels of ROS under heat, drought, chilling, Cd toxicity and short photoperiod stresses, mutant lines, especially double and triple mutants would show hypersensitivity compared to the wild-type. Based on the performance and susceptibility of each mutant line under different abiotic stresses, novel functions for Class II GRXs were proposed.

MATERIALS AND METHODS

Selection of target sequences and vector construction

Two sequences on each *SIGRXS14* (*S14*), *SIGRXS15* (*S15*), *SIGRXS16* (*S16*), and *SIGRXS17* (*S17*) genes were targeted by the multiplex CRISPR/Cas9 system. Guide RNAs were designed using CRISPR-P 2.0 website (<http://crispr.hzau.edu.cn/CRISPR2/>). The specificity of the guides was confirmed by Blast search of guide sequences against the tomato genome (<http://blast.ncbi.nlm.nih.gov/Blast.cgi>). Sequences with at least two mismatches within the PAM region and five mismatches in the PAM-distal region were targeted (Jinek et al., 2012). Among those, guides with the highest score, meaning least off-target edit possibilities were selected. Each single guide RNA (sgRNA) was driven by an AtU6 promoter and 8 “T” terminator. All sgRNAs along with their promoter and terminator were assembled into a single gRNA (sgRNA) array. sgRNA array was synthesized and cloned into pYLCRISPR/Cas9-P35S-N binary vector (**Figure 2-1**). The CRISPR/Cas9 construct was transformed into Top 10 chemically competent *E. coli* cells (Thermo Fisher Scientific, MA, USA) and the transformation was confirmed by both antibiotic selection and the kanamycin PCR using KAN marker designed on NPTII sequence. Vectors were then transformed into *Agrobacterium tumefaciens* strain LBA4404 using the freeze-thaw method (Holsters et al., 1978) and confirmed by both antibiotic selection and kanamycin PCR using KAN marker designed on NPTII sequence.

Plant transformation

pYLCRISPR/Cas9-P35S-N binary vector was transformed into tomato using *Agrobacterium*-mediated transformation as described previously (Park et al., 2003). Briefly, surface-sterilized seeds were germinated on Murashige and Skoog (MS) (Murashige and Skoog, 1962) inorganic salt medium containing 30 g⁻¹ sucrose (pH 5.7) and 8 g⁻¹ agar (PhytoTechnology, KS, USA).

Hypocotyls and cotyledons of *in vitro* grown very young tomato seedlings before the appearance of true leaves were excised and precultured on MS inorganic salts with 100 mg^l-1 inositol, MS vitamins, 30 g^l-1 sucrose, 0.1 mg^l-1 naphthalene acetic acid, 1 mg^l-1 6-benzyl-aminopurine and 8 g^l-1 agar for 1 day. Then, explants were inoculated with *Agrobacterium* for 1 min and re-cultured on the same medium for three days. Explants were afterward transferred on selection medium with MS inorganic salts, 30 g^l-1 sucrose, 100 mg^l-1 inositol, MS vitamins, 2 mg^l-1 zeatin, 0.1 indole-3-acetic acid, 100 mg^l-1 kanamycin, 250 mg^l-1 Clavamox® (Zoetis, NJ, USA) and 8 g^l-1 agar. Cultures were kept at 22°C with continuous light for 6–8 weeks for shoot regeneration with every two weeks sub-culturing, then shoots were transferred into rooting medium containing MS inorganic salt medium, 30 g^l-1 sucrose (pH 5.7), 100 mg^l-1 kanamycin, 250 mg^l-1 Clavamox and 2 g^l-1 Gelzan™ (PhytoTech Labs, KS, USA) for another 6 weeks. Tomato seedlings were afterward established in soil and moved to growth chambers at 20–25°C with a 14-h photoperiod. The plants were watered once every week with Miracle-Gro® Tomato Plant Food (ScottsMiracle-Gro, NY, USA).

DNA isolation, transgenic screening and genotyping

Genomic DNA from wild-type and T0, T1, and T2 transgenic tomato leaves was extracted using 2% cetyltrimethylammonium bromide (CTAB) buffer containing 2% cetyl trimethylammonium bromide, 1% polyvinyl pyrrolidone, 100 mM Tris-HCl, 1.4 M NaCl, 20 mM EDTA. Tomato leaves were ground to a fine powder using liquid nitrogen and mixed with 400 µl of 2% CTAB buffer and 4 µl of DNase free RNase I (Thermo Fisher Scientific, MA, USA). Samples were incubated in 55 °C water bath for 30 min, then mixed with 400 µl of phenol:chloroform:isoamyl alcohol (25:24:1), and centrifuged for 10 min at 13000 rpm. 400 µl isopropanol and 80 µl 3 M sodium acetate were added to the supernatant and centrifuged for 10 min at 13000 rpm. DNA

pallets were washed with 70% ethanol for 3 times and diluted with sterilized water. To confirm the integration of the T-DNA region into T0 transgenic plants kanamycin PCR using KAN marker designed on NPTII sequence was performed. To screen for transgene-free mutant lines in T1 plants, PCR using Cas9 and KAN markers was performed. For genotyping, genomic target sites in T0, T1, and T2 mutant lines were PCR amplified and sequenced by Sanger sequencing. Sequencing reads were analyzed using Sequencher software. All primer sequences are listed in **Table 2-1**.

Heat stress assay

T3 *s14*, *s16*, and *s17* single mutants, *s14::16* double mutant, *s14::16::17* triple mutant, and wild-type plants were grown in 4-inch pots filled with Metro-Mix (Sun Gro Horticulture Canada Ltd) and kept in growth chamber with 24/20 °C day and night temperature under 12 h photoperiod. Light intensity was 300 $\mu\text{mol photons m}^{-2}\text{s}^{-1}$. Plants were watered daily and fertilized regularly using Miracle-Gro® Tomato Plant Food (ScottsMiracle-Gro, NY, USA). Four-weeks-old tomato seedlings were exposed to 38/28 °C day and night temperatures for three days, continued by 45/35 °C day and night temperatures (Camejo et al., 2005; Wu et al., 2012) for 10 days to see phenotypic differences between genotypes. Three independent experiments were performed, and each experiment included six replications per genotype per treatment.

Drought stress assay

T3 *s14*, *s16*, and *s17* single mutants, *s14::16* double mutant, *s14::16::17* triple mutant, and wild-type plants were grown in 4-inch pots filled with Metro-Mix (Sun Gro Horticulture Canada Ltd) and kept a in growth chamber with 24/20 °C day and night temperature under 12 h photoperiod. Light intensity was 300 $\mu\text{mol photons m}^{-2}\text{s}^{-1}$. Plants were watered daily and fertilized using Miracle-Gro® Tomato Plant Food (ScottsMiracle-Gro, NY, USA) as required. Four-weeks-old

tomato seedlings were subjected to drought stress by withholding water for 15 days and recovered by watering for a week. Before drought treatment, at day 0, all pots were saturated with water and drained three times to make sure they all are at the pot capacity and contain same amount of water. Two independent experiments were performed, and each experiment included six replications per genotype per treatment.

Chilling stress assay

T3 *s14*, *s16*, and *s17* single mutants, *s14::16* double mutant, *s14::16::17* triple mutant, and wild-type plants were grown in 4-inch pots filled with Metro-Mix (Sun Gro Horticulture Canada Ltd) and kept in a growth chamber with 24/20 °C day and night temperature under 12 h photoperiod. Light intensity was 300 $\mu\text{mol photons m}^{-2}\text{s}^{-1}$. Plants were watered daily and fertilized using Miracle-Gro® Tomato Plant Food (ScottsMiracle-Gro, NY, USA). Four-weeks-old tomato seedlings were subjected to 4 °C day and night temperature for four weeks and were recovered at 24/20 °C day and night temperatures for one week. Three independent experiments were performed, and each experiment included six replications per genotype per treatment.

Cadmium toxicity assay

T3 *s14*, *s16*, and *s17* single mutants, *s14::16* double mutant, *s14::16::17* triple mutant, and wild-type tomato seeds were surface-sterilized by soaking in 10% Clorox and one drop of Tween20 for 30 min and rinsed with sterilized water for three times. Sterilized seeds were placed on MS media (Murashige and Skoog, 1962) to germinate under continuous light at 24 °C. Half of the uniformly germinated seeds were moved to vertical plates containing MS media with 50, 100, and 150 μM concentrations of cadmium sulfate, and the other half was moved to MS media as control. The root length of seedlings was measured after one week. Three independent experiments were done, and each experiment included eight replications per genotype per treatment.

Photoperiod and nutrient assays

Growth chamber experiments

Germinated seedlings of T3 *s14*, *s16* and *s17* single mutants, *s14::16* double mutant, *s14::16::17* triple mutant, and wild-type plants were transferred to 4-inch pots filled with Metro-Mix (Sun Gro Horticulture Canada Ltd) and kept in growth chambers with the light intensity of 300 $\mu\text{mol photons m}^{-2}\text{s}^{-1}$ at 24 °C under long (16 h), control (12 h), and short (8 h) photoperiods. Three independent experiments were done, and each experiment included six replications per genotype per treatment. Seedlings were randomly assigned to the treatments.

Greenhouse experiments

Germinated seedlings of T3 *s14*, *s16* and *s17* single mutants, *s14::16* double mutant, *s14::16::17* triple mutant, and wild-type plants were transferred to 4-inch pots filled with Metro-Mix (Sun Gro Horticulture Canada Ltd) and moved to the greenhouse with 24/20 °C day and night temperatures. For the control group, tomato seedlings were kept under natural greenhouse light at ~12 h photoperiod and fertilized every week with 250 ml of Miracle-Gro® Tomato Plant Food (ScottsMiracle-Gro, NY, USA). For short photoperiod group, tomato seedlings were covered every day at 5 pm and uncovered at 9 am to receive only 8 h of day light. Seedling were regularly fertilized. For nutrient deficiency group, tomato seedlings were kept under natural greenhouse light at ~12 h photoperiod and fertilized only once with 250 ml of Miracle-Gro® Tomato Plant Food at the time of plant establishment. For the combined-short photoperiod and nutrient deficiency group, tomato seedlings received 8 h of day light and were fertilized only once. Eight replications per genotype were used for each treatment group. Tomato seedlings were randomly assigned to each treatment in a completely randomized design. Shoot fresh weight and flowering

time were measured. Data were analyzed using three-way ANOVA with IBM SPSS software (IBM Corp.)

RESULTS

Characterization of CRISPR/Cas9 targeted mutations in T0 transgenic plants

A total number of 10 independent transgenic lines (T0 generation) were regenerated. CRISPR/Cas9 T-DNA insertion into genomic DNA was confirmed by PCR using kanamycin primers listed in **Table 2-1**. Genomic regions comprising target sites were PCR amplified and sequenced to detect mutations using Sanger sequencing analyses are shown in (**Figure 2-2a**). With the average transformation efficiency of 60%, of the 10 T0 transgenic lines, 6 had mutations for target genes. Multiplex editing of four genes resulted in one double mutant (line #9), three triple mutants (lines #2, 10, and 11), and two quadruple mutants (lines #1 and 3) in T0 generation (**Table 2-2**). gRNAs differed in their editing efficiency and their average efficiency was 12.5% (**Table 2-3**). In T0 generation 86% of mutation were heterozygous mutations and 14% of mutations were chimeric mutations. Chimeric mutations or chimeric plants are composed of genetically distinct cells. In addition to the transformed cells, chimeric plants include non-transformed cells that could be created as a result of protection from the kanamycin resistance transformed cells during regeneration. Chimeric plants produce non-transformed gametes and cannot induce stable edits (Chen, 2011). While heterozygous mutations give rise to stable edits. Chimeric plants were eliminated from further analysis. Of the heterozygous mutations, 23%, 23%, 33%, and 4% of mutations were 1 bp insertions, 1 bp deletions, small deletions, and big deletion, respectively (**Figure 2-2b**). Deletion mutations ranged from 1 bp up to 210 bp. Among all modifications, 1 bp insertion had the highest frequency (**Figure 2-2a**). Frequencies of deletions and insertions for each one of A, T, C, and G bases were 21%, 27%, 33%, and 19%, respectively (**Figure 2-2c**).

Inheritance and stability of targeted mutations in T1 and T2 mutant lines

To evaluate heritability of Cas9/gRNAs induced genomic mutations, selected T1 and T2 transgenic plants obtained from self-fertilized T0 transgenic lines #2, #3, and #10 were genotyped by sequencing. Before proceeding with genotyping, progenies from selected lines were screened to obtain CRISPR/Cas9-free (T-DNA free) plants to prevent further edits on wild-type genes and stabilized single, double, triple and quadruple mutants. To screen CRISPR/Cas9-free plants, 50 T1 seedlings from each selected T0 line were grown and screened for the presence of T-DNA using Cas9 PCR (**Supplementary Figure 2-1**). About 20% of the screened plants from each line were Cas9 negative, which is CRISPR/Cas9-free. T-DNA free plants from each line were subjected to genotyping by sequencing PCR amplified target regions. In examined lines, all T0 genotypes transmitted to T1.

Line #2 which harbored heterozygous mutations for *S15*, *S16*, and *S17* in T1 generation was segregated to produce ratios of 0:0:1, 0:1:0, and 1:0:3 for alleles of each gene, respectively. All tested progeny carried 5 bp (AACTG), and 6 bp (AATGGC) deletions in *S16* and *S17* genes, respectively, corresponding to the same T0 mutations. No mutant allele was detected for the *S15* gene in T1 progeny. Mutated and wild-type *S14*, *S15*, *S16*, and *S17* alleles of line #3 were segregated with ratios of 2:2:1, 0:2:3, 2:7:1, and 1:7:1 in the T1 generation, respectively. Mutated alleles of *S14*, *S15*, *S16*, and *S17* carried 2 bp deletion (GA), 1 bp insertion (T), 7 bp deletion (GCTCACC), and 1 bp insertion (T), respectively as observed in T0 generation. However, one exception occurred in one of the plants which contained 1 bp T insertion in the *S16* mutant allele, instead of the original 7 bp deletion. T1 progeny of line #10 were segregated with ratios of 1:2:0, 0:3:3, and 1:1:4 for *S14*, *S15*, and *S16* wild-type and mutated alleles, respectively. Each mutant

allele contained the same mutation as T0 mutant alleles including 1 bp (A) and (C) deletion for *S14* and *S16* respectively, and 1 bp (T) insertion for *S15* (**Table 2-4**).

T1 plants contained both homozygous and heterozygous mutations. Four T-DNA free T1 lines obtained from the three selected T0 lines (#2-1, #3-9, #10-3, and #10-4) were self-fertilized to obtain T2 homozygous mutations with all mutant alleles. T2 progenies were genotyped by sequencing PCR amplified target regions of each gene. Genotyping data indicated the same edits were transmitted from T1 to T2 plants, confirming stable heritability of mutations from second to the third generation as well. However, segregation of genes did not follow the Mendelian ratio in some lines. T2 progenies of line #2-1, which contained homozygous mutation for *S17* and heterozygous mutation for *S16* in T1 generation, showed only homozygous mutation for *S17* as expected, but all of 11 examined T2 plants were null for *S16*. T2 progenies of line #3-9 which harbored homozygous mutations for *S14*, *S16*, and *S17* in T1 generation, and heterozygous mutation for *S15*, were segregated with a ratio of 0:1:1 for *S15* and all homozygous for the other three genes as expected. Out of 14 plants genotyped none of them contained homozygous mutations of *S15*, indicating that *S15* loss of function is embryonic lethal. T2 progenies of line #10-3, which had homozygous edits for *S16* and heterozygous edits for *S14* were segregated with a ratio of 2:5:2 for *S14* and all homozygous for *S16* as expected. T2 progenies of line #10-4, which contained heterozygous edits for both *S14* and *S15* were segregated with a ratio of 7:13:3 for *S14* and 0:9:14 for *S15*. No progeny with homozygous mutation for *S15* was observed, confirming *S15* homozygous mutants are embryonic lethal (**Table 2-5**). Transgene-free individuals containing only homozygous mutations of *s14*, *s16*, and *s17* were selected and their T3 seeds were harvested for subsequent phenotypic experiments.

***Slgrx* null mutants have reduced heat tolerance**

To determine the importance of class II GRXs for tomato's response to high temperatures *s14*, *s16*, and *s17* single mutants, *s14::16* double mutant, *s14::16::17* triple mutant, and wild-type plants were exposed to high temperatures. Under normal condition, 18 individuals of each mutant line and wild-type did not show any visually phenotypic differences (**Figure 2-3a**), while all single, double, and triple mutant lines showed impaired growth under heat stress. *s14* and *s17* single mutants were heavily affected by heat stress and showed severe heat stress symptoms such as burned leaves and slowed growth, while *s16* single mutants showed less severe heat stress symptoms. Due to the added impact of *s14*, *s16*, and *s17* mutations, triple mutant plants showed the most severely impaired growth. Phenotyping data showed that *s14* and *s17* single mutants and *s141617* triple mutant tomato plants are very sensitive to heat stress and cause lethality in seedlings (**Figure 2-3b**).

***Slgrx* null mutants have reduced drought resistance**

To study the impact of class II GRXs on plant's response to drought stress, *s14*, *s16*, *s17* single mutants, *s14::16* double mutant, *s14::16::17* triple mutant and wild-type plants were subjected to drought stress by withholding water for 15 days. All 9 individuals of each mutant line and wild-type did not show any visually phenotypic differences at day 0 (control) (**Figure 2-4a**), while, *s17* mutant line showed the highest degree of drought stress symptoms such as wilting followed by wild-type at day 15. The rest of the lines showed minor drought stress symptoms (**Figure 2-4b**). After recovering plants by regular watering for one week, *s17* single mutant and wild-type tomatoes did not recover and died, while the rest of the lines completely recovered (**Figure 2-4c**).

***Slgrx* null mutants have reduced chilling tolerance**

To investigate the functions of class II GRXs in response to low-temperature in tomato, *s14*, *s16*, and *s17* single mutants, *s14::16* double mutant, *s14::16::17* triple mutant, and wild-type plants were subjected to chilling stress. Under normal condition, 18 individuals of each mutant line and wild-type did not show any visually phenotypic differences (**Figure 2-5a**). However, under chilling treatment *grx* mutant lines showed more severe chilling stress symptoms such as stunt growth and wilting compared to wild-type after 10 days (**Figure 2-5b**). Consistently, after one week of recovery under optimal temperature, wild-type plants were completely recovered, while none of the *grx* mutant lines were recovered (**Figure 2-5c**).

***Slgrx* null mutants have reduced growth under cadmium toxicity**

Uniformly germinated wild-type and *s14*, *s16*, *s17* single mutants, *s14::16* double mutant, and *s14::16::17* triple mutant lines were grown on MS media containing Cd and their growth and root length was measured to evaluate the function of class II GRXs in heavy metal toxicity tolerance.

Wild-type and mutant line did not show significant difference in their root length under control condition compared to 50 and 100 μM Cd toxicity conditions. Wild-type plants did not show any significant differences in their root length grown on MS media with or without Cd. While *s14*, *s16*, and *s17* single mutants, *s14::16* double mutants, and *s14::16::17* triple mutants had reduced root length when grown under 150 μM Cd toxicity condition compared to the control condition. *s17* single mutant and subsequently *s14::16::17* triple mutant had smaller root length compared to wild-type even under control condition, however, under Cd toxicity condition, root length reduction was more severe (**Figure 2-6a, b**).

***Slgrx* null mutants have reduced growth and delayed flowering under short photoperiod**

Growth chamber experiments

Sl7 is involved in plants' response to long photoperiods (Knesting et al., 2015). To further investigate function of class II GRXs in tomato's response to different photoperiods, wild-type and *s14::16::17* triple mutant plants were grown under short (8 h), medium (12 h), and long (16 h) photoperiods for two months. Tomato seedlings of wild-type and *s14::16::17* triple mutant did not show any phenotypic differences when grown under 12 h and 16 h photoperiods. *s14::16::17* triple mutants showed very retarded to almost lethal phenotype when grown under 8 h photoperiod (**Figure 2-7a**).

Next, to find which single mutant(s) caused severe retarded phenotype in *s14::16::17* triple mutant under short photoperiod, further phenotypic analyses were performed using *s14*, *s16*, and *s17* single mutants and *s14::16* double mutant in addition to *s141617* triple mutant under 8 h photoperiod. Since no phenotypic difference was observed within 16 h and 12 h photoperiods, 16 h photoperiod was eliminated from further studies and 12 h photoperiod was selected as control. When grown under 12 h photoperiod none of the mutant lines showed noticeable phenotypic differences (**Figure 2-7b**). When grown under 8 h photoperiod, *s14* and *s17* single mutants showed reduced growth compared to wild-type, while *s16* single mutants did not show any growth defects, indicating that the severe growth defects observed in *s14::16::17* triple mutants are caused by cumulative effects of *s14* and *s17* single mutants (**Figure 2-7c**).

Greenhouse experiments

The response of wild-type and mutant lines to different photoperiods was also evaluated in greenhouse condition. Results from the greenhouse trial were consistent with growth chamber

experiments. No phenotypic difference was observed among wild-type and mutant lines under 12 h photoperiod. While under 8 h photoperiod *s14* and *s17* single mutants and subsequently *s14::16::17* triple mutant showed very poor phenotypes (**Figure 2-8a**). Accordingly, wild-type and mutant lines did not show significant differences in shoot fresh weight of seedlings under 12 h photoperiod, while mutant lines had up to ~5 times reduction in shoot fresh weight under 8 h photoperiod (**Figure 2-9a**).

Also, to test whether short photoperiod increases mutants' sensitivity to nutrient limitation, half of the plant under each photoperiod was subjected to nutrient deficiency by withholding fertilizer application. Under short days, ROS levels increase. While, sufficient fertilizer specially nitrogen, can enhance antioxidant system, which is already weekend due to mutations in class II GRXs, leading to reduced oxidative damage and higher photosynthesis rate. So, we hypothesized that sufficient fertilization can compensate for the restarted growth that was induced by short days in mutant lines (Medici et al., 2004). Phenotypes under 12 h photoperiod showed that *s14* and *s141617* mutants were more sensitive to low nutrient access compared to wild-type (**Figure 2-8b**). Consistently, *s14* single mutant and *s14::16::17* triple mutant showed reduced shoot fresh weight compared to wild-type when faced with nutrient deficiency (**Figure 2-9b**). By withholding fertilizer under 8 h photoperiod, *s14* and *s17* single mutants and *s14::16::17* triple mutants showed very weak phenotype and had significant reduction in shoot fresh weight. Data analysis using three-way ANOVA showed that shoot fresh weight was associated with genotype, nutrient, photoperiod, genotype * nutrient, genotype * photoperiod, nutrient * photoperiod, and genotype * nutrient * photoperiod. Further analysis using student's *t*-test showed that more mutant lines are sensitive to short photoperiod than limitation in nutrients (**Table 2-6**).

The flowering time of wild-type and mutant lines was counted under 8 and 12 h photoperiods with both sufficient and low fertilizer applications. The day that first flower on each plant started to open was counted as the flowering date. Three-way ANOVA analysis of data showed that flowering time is associated with genotype, nutrient, photoperiod, genotype * photoperiod, nutrient * photoperiod (**Table 2-7**). Under 12 h photoperiod and sufficient nutrients (control condition), wild-type and *s16* single mutant started flowering on the same day, while *s14* single mutant, *s17* single mutant, *s14::16* double mutant and *s14::16::17* triple mutant had delayed flowering by 9, 9, 2 and 6 days, respectively (**Figure 2-10a & b**). Under 12 h photoperiod without nutrient deficiency *s14* and *s17* single mutants had delayed flowering by 5 and 6 days, respectively, while *s16* single mutant and *s14::16* double mutant started to flower 3 days before wild-type. The *s14::16::17* triple mutant did not show flowering delay and started the flowering same day as wild-type (**Figure 2-10c & b**).

Under 8 h photoperiods, with both sufficient and low fertilizer applications *s14* single mutant and *s14::16::17* triple mutant seedlings had severe growth and development defects and never entered the flowering stage. *s17* single mutants showed delayed flowering only when grown with sufficient nutrient, while, *s14::16* double mutants had delayed flowering only when grown with nutrient deficiency. On the other hand, *s16* single mutant started to flower few days before wild-type (**Figure 2-10d, e & f**).

DISCUSSIONS

In this study, we successfully designed and applied the pYLCRISPR/Cas9 multiplex vector system to edit four members of class II GRX genes, *S14*, *S15*, *S16*, and *S17* in tomato and used mutant lines to study functions of knocked out genes under several abiotic stress conditions. Our genotyping data showed high-efficiency gene editing in T0 plants that were genetically inherited to T1 and T2 generations. For some lines, segregation of wild-type and mutant alleles followed the Mendelian ratio, but for some lines it did not. Maybe a bigger sample size would have resulted in different ratios. After creating edits, CRISPR/Cas9 construct was eliminated from mutant lines by segregation in the next generations to avoid any further edits on wild-type alleles. Unsuccessful attempts to find any single, double, triple, or quadruple mutant lines containing *s15* homozygous mutants indicate that complete loss of function of *S15* is embryonic lethal. *s15* Arabidopsis homozygous mutants also showed embryo abortion at an early stage after fertilization (Moseler et al., 2015). *S15* is exclusive and the only or the major GRX in mitochondria involved in iron-sulfur cluster assembly as a scaffold protein, hence its loss of function can severely affect important tricarboxylic acid cycle and subsequently electron transport chain enzymes which contain iron-sulfur clusters and located in mitochondria (Ströher et al., 2016). Our data supports vital functions for *S15* in mitochondria, and suggests its function is probably conserved across all species. Phenotyping experiments were carried out with five homozygous mutant lines including *s14*, *s16*, and *s17* single mutants, *s1416* double mutant and *s141617* triple mutant. Mutant lines were evaluated under control, heat, drought, chilling, cadmium toxicity, and short photoperiod stress conditions. Under the control condition, *s14*, *s16*, and *s17* single mutants, *s1416* double mutant, and *s141617* triple mutant lines did not show any significant phenotypic differences compared to wild-type plants. The indistinguishable phenotype of mutant lines suggests that the function of

S14, *S16* and *S17* GRXSs is not required for tomato's normal growth and development under control conditions. In contrast to the control condition, upon exposure to different abiotic stresses wild-type and mutant plants showed significant phenotypic differences that were readily distinguishable.

Heat stress

When grown under high temperature all class II GRX mutant lines showed more severe heat stress symptoms compared to wild-type (**Figure 2-3b**). Extreme poor phenotypes observed in *s14* and *s17* single mutants suggest that these genes are critical mediators of tomato's response to heat stress. Our data propose that there is no functional redundancy between *S14*, *S16* and *S17* GRXs in tomato's response to heat stress. The response of chloroplastic redox regulators to heat stress is independent of cytosolic or nuclear response because none of the chloroplastic GRXs could complement cytosolic *s17* loss of function and vice versa. Moreover, there is no functional redundancy between the two chloroplastic GRXs because none of the *s14* or *s16* single mutants showed a wild-type phenotype. *s14* mutant tomatoes were more heat sensitive than *s16* mutants. Severely damaged double mutant plants and lethal phenotype observed in triple mutant plants suggest that loss of function effects of GRXs are cumulative and all three class II GRXs are required for tomato's heat stress response. Cytoplasmic *S17* is involved in tomato's response to high temperatures through increased expression of heat shock proteins (HSPs) and catalase enzyme resulted in reduced H₂O₂ accumulation without yield loss (Hu et al., 2015; Wu et al., 2012). In Arabidopsis, the high temperature increased expression levels of *AtGRXS17*, and also *Atgrxs17* knock down lines showed higher sensitivity in response to heat stress (Hu et al., 2015; Wu et al., 2012). Moreover, expression of *AtGRXS17* in yeast *grx3grx4* double mutants which are heat sensitive positively affected their survival under heat stress (Wu et al., 2012). However, there

have not been any studies reporting involvement of chloroplastic *S14* and *S16* GRXs in plant's response to high temperatures and our research is the first to show *S14* and *S16* GRXs are heavily involved in heat stress response in plants. Heat stress activates morphological, physiological and molecular responses in plants. The molecular response includes 1) induced oxidative stress and antioxidants, and 2) expression of stress proteins such as (HSPs). The ability of plants to protect themselves against induced oxidative stress can determine plant's survival under heat stress (Wahid et al., 2007), and *S17* is proved to be involved in redox regulation during heat stress through both ROS scavenging and inducing expression of stress proteins responses (Hu et al., 2015; Wu et al., 2012). However, how chloroplastic GRXs, *S14* and *S16* respond to heat stress still remains to be uncovered. *AtGRXcp*, which is a CGFS monothiol GRX localized in chloroplast, complemented the phenotype of yeast *grx5* mutants when exposed to H₂O₂. Yeast *grx5* mutants are sensitive to oxidative stress and contain increased levels of protein carbonylation. *AtGRXcp* expressing yeast mutants showed decreased protein carbonylation. Suggesting that *AtGRXcp* can protect oxidative damage to proteins (Cheng et al., 2006). Moreover, loss of function of *Atgrxcp* increased sensitivity of seedlings to oxidative damage (Cheng et al., 2006). Heat stress also causes oxidative damage to the proteins (Sundaram and Rathinasabapathi, 2010). Thus, tomato's chloroplastic monothiol GRXs, *S14* and *S16* may also be involved in heat tolerance response by decreasing protein carbonylation caused by heat stress. Given the critical functions of both cytosolic and chloroplastic GRXs for tomato's survival under high temperature, it is possible that *S14* and *S16* GRXs are involved in heat tolerance response in chloroplast by decreasing carbonylation of chloroplastic proteins, and *S17* is involved in nuclear and cytoplasmic heat tolerance response (Hu et al., 2015; Wu et al., 2012).

Drought stress

Ectopic expression of *AtGRXS17* increased tomato's resistance to drought stress by reducing excessive ROS accumulation and regulating stress responsive genes (Wu et al., 2017). Consistently, *s17* single mutant plants were severely damaged under drought, confirming importance of *S17* in tomato's response to drought stress. However, despite our expectations (higher drought sensitivity in mutant lines due to high ROS accumulation as a result of less antioxidant activity), *s14* and *s16* single mutants showed higher drought resistance compared to wild-type, and also complemented *s17* loss of function in triple mutants (**Figure 2-4**). Chloroplastic *S14* and *S16* might be involved in photosynthesis. Their loss of function may have resulted in lower photosynthesis rate which reduces plants' needs for water, causing higher drought resistance. Higher drought resistance of class II GRX knocked down lines was also observed in *O_sGRXS17*-RNAi rice as a result of stomata closure and increased water content (Hu et al., 2017).

Chilling stress

When subjected to chilling stress all single, double, and triple mutants were severely affected. Our data indicate that functions of each of *S14*, *S16*, and *S17* monothiol GRXs, are critical for tomato's response to chilling stress, regardless of the presence or absence of the other monothiol class II GRXs. Our phenotyping data propose that there is no functional redundancy between *S14*, *S16* and *S17* in tomato's response to chilling stress because the phenotype of none of the single mutants could be complemented with the function of the other two GRXs (**Figure 2-5**). *S14*, *S16* and *S17* may contribute to tomato's chilling stress response through three independent vital mechanisms, or they all could be vital components of the same chilling response mechanism. Overexpression of *S17* and its relocation to the nucleus increased tomato's tolerance to chilling probably through nucleus signaling followed by decreasing ion leakage, H₂O₂ accumulation, and increasing soluble

sugar, photochemical efficiency and antioxidant enzyme activities (Hu et al., 2015). *S14*, on the other hand, may also be involved in the response to chilling stress through brassinosteroid-mediated chilling tolerance by maintaining redox homeostasis of chloroplast in tomato (Xia et al., 2018). Despite the lethal phenotype of *s16* mutants observed in this work and the impact that *S16* may have on tomato's chilling tolerance, there have not been any studies investigating *S16* under chilling stress. Thus, involvement in chilling stress is a novel function of *S16* reported in this research. Chilling stress can cause damage to the plant by inhibiting its growth or by direct damage to the cells. In cold sensitive plants such as tomato even a mild chilling stress can cause up to 50% yield reduction due to reduced photosynthesis and increased respiration rate (Lukatkin et al., 2012). The reduced photosynthesis happens as a result of lipid peroxidation in chloroplast membrane caused by excess ROS (Kingston-Smith & Foyer, 2000). ROS accumulation during chilling stress happens as a result of reduced antioxidant system (Alam & Jacob, 2002). Possibly already deteriorated antioxidant system due to chilling stress accompanied with loss of function of *S14*, *S16* and/or *S17* oxidoreductases may cause lethality in mutant lines.

Cadmium toxicity

The severe effect of Cd toxicity on root growth of *s17* single mutant and subsequently *s14::16::17* triple mutant compared to wild-type suggests that *S17* GRX is heavily involved in tomato's response to Cd toxicity stress. *s14* and *s16* single mutants showed slightly smaller root length compared to wild-type, while *s14::16* double mutant showed more severe reduction in root length probably as a result of cumulative effects of both *s14* and *s16* single mutants, suggesting that the two chloroplastic class II GRXs, work together to protect chloroplasts from Cd toxicity. Our data showed that *S17* is critical and the most important class II GRX for tomato's growth and development under Cd toxicity condition followed by *S14* and *S16*. Regardless of presence or

absence of *S14* and *S16*, loss of function of *S17* in both single and triple mutants caused very small root phenotype, suggesting that function of *S17* is independent from *S14* and *S16*, while functions of *S14* and *S16* could depend on *S17* (**Figure 2-6a & b**).

Increased activities of *GRXS12* and *GRXC4* of germinating pea seeds exposed to high Cd concentrations further highlights the importance of GRXs in heavy metal toxicity response (Smiri et al., 2011). In yeast expression levels of *GRX2* increased in response to Cd treatment (Vido et al., 2001). Expression of Fern *Pteris vittata* *GRX5* reduced accumulation of arsenite levels in bacteria (Sundaram et al., 2008), and arsenic levels in *Arabidopsis* (Sundaram et al., 2009). Moreover, *AtGRXS15* is involved in reducing arsenic levels and increasing tolerance in *Arabidopsis* (Ströher et al., 2016). The function of class II GRXs in Cd toxicity response in higher plants has not been well studied, and the *Slgrx* mutant lines established here are a valuable source for more in depth studies of Cd toxicity tolerance mechanisms in plants. Moreover, based on phenotyping results, overexpression of class II GRXs, specially *S17* in crops could increase their tolerance to Cd toxicity. Plants with a higher Cd toxicity tolerance have lower Cd content reducing Cd entrance to human food chain (Wang, 2002). Cd tolerant plants may immobilize Cd ions at root tissues, hence increasing their tolerance to grow in soil with high concentrations of Cd. Alternatively, they might use detoxification mechanism after Cd is already taken up by the plant (Das et al., 1997). Detoxification or inhibiting Cd mobilization could prevent heavy metals from entering the food chain. Excessive application of pesticide and fertilizer, mining, natural soil properties are among the causes of heavy metal toxicity such as high aluminum, manganese, iron, and Cd. Cd can be taken up by plants and enter the food chain thus has been subjected to many studies (Das et al., 1997; Foy et al., 1978)

Photoperiod

The photoperiod experiments showed that *S14* and *S17* are critical for tomato's development and flowering under 8 h short photoperiod and also on-time flowering under 12 h photoperiod (**Figure 2-10a-f**). *s14* single mutants did not even enter the flowering stage under short photoperiod, which could be, in part, due to small and undeveloped growth observed in seedlings. However, delayed flowering of *s14* single mutants under 12 h photoperiod with normal phenotype, suggests that not only *S14* is critical for vegetative growth and reproductive development under short photoperiod, but also it is tightly involved in reproductive growth under 12 h photoperiod. Three-way ANOVA analysis indicate that photoperiod * nutrient * genotype interaction is statistically significant at fresh weight (**Table 2-6**) but not flowering time (**Table 2-7**). The extreme phenotype observed in *s14* single mutants and subsequently *s14::16::17* triple mutant (**Figure 2-9a & b**) could be because *S14* is the only enzyme that controls deglutathionylation in the chloroplast (Lemaire et al., 2007). Many important enzymes in chloroplast including those involved in the Calvin cycle require deglutathionylation, suggesting functional importance of *S14* in the Calvin cycle and photosynthesis especially under stress condition (Zaffagnini et al., 2008). Consistently, our data confirmed that *S14* is the only chloroplastic deglutathionylation GRX enzyme, since *S16* did not complement *s14* single mutants (**Figure 2-9a & b**). This finding suggests that there is no interplay between the two chloroplastic GRXs in tomato's growth and flowering in response to short photoperiod, and only one chloroplastic GRX, *S14*, is for development of tomato seedlings and flowers under short photoperiod. In *Arabidopsis*, upon exposure to dark treatment, *S14* was found to be more oxidized, and *Ats14* mutants had a low chlorophyll content, both proposing *S14* is involved in plant's response to light related environmental stresses and its absence causes an imbalance in redox status (Rey et al., 2017). *s17* mutants also showed delayed flowering under

both short and long days. delayed flowering in *s17* mutants was also observed in *Arabidopsis* (Knesting et al., 2015). Accordingly, overexpression of *AtGRXS17* in chrysanthemum induced faster flowering (Kang et al., 2019). *S17* may be involved in maintaining shoot apical meristem, cell proliferation and differentiation (Schippers et al., 2016) and subsequently affecting flowering time by regulating auxin signaling transduction pathway (Cheng et al., 2011) and/or NF-YC11/NC2 α activity (Knesting et al., 2015). In contrast to delayed flowering observed in *s14* and *s17* mutants, *s16* mutants showed prompt flowering under short photoperiods compared to wild-type plants. Our findings suggest that *S16* could be a negative regulator of flowering unlike *S14*, and they may have opposite effects causing intermediate phenotype observed in *s14::16* double mutant plants.

CONCLUSIONS

We generated inheritable single and multiple *Slgrxs* mutants using CRISPR/Cas9 system and demonstrated that loss of function of class II GRX members, causes hypersensitivity in tomato plants under heat, drought, chilling, Cd toxicity and short photoperiods, and proposed novel functions for *S14*, *S16* and *S17* GRXs. A summary of our phenotyping data is shown in **table 2-8**. Oxidative stress caused as a result of abiotic stress conditions disturbs photosynthesis which leads to limitations in the electron transport chain and NADPH production. Thioredoxins (TRX), which are one of the two main redox systems of the cell, uses NADPH as a reducing substance to fight oxidative stress (Gillet et al., 2006; Yang & Ma 2010). However, decrease in NADPH content under abiotic stress conditions, probably limits thioredoxin activity. Thus, under stress conditions, function of the other redox system, GRXs, especially monothiol class II GRXs which use GSH instead of NADPH as reducing substance becomes vital. That can be one reason why under stress conditions, mutants lacking class II GRXs showed more severe stress symptoms and impaired growth compared to wild-type plants containing both GRX and TRX redox systems. Furthermore, the chloroplast is a very sensitive organelle to ROS imbalances because even small excess amounts of ROS in chloroplast can inhibit photosynthesis by 50%, thus redox regulation in the chloroplast is very critical (Duan et al., 2012). This could explain the consistent severe poor phenotype observed in mutants lacking chloroplastic *S14* under multiple abiotic stresses such as short photoperiod, cadmium toxicity, heat, and chilling. Not only class II GRXs are involved in response to several abiotic stresses, but also, they are involved in plant development mechanisms such as flowering through redox regulation. These mutant lines generated here are a valuable resource to study physiological and molecular mechanisms of heat, drought, chilling, Cd toxicity, and short photoperiod stresses. Our results suggest monothiol class II GRXs studied in this

research especially *S14* and *S17* are ideal candidates to be overexpressed in important food crops to improve their tolerance to multiple abiotic stresses. Class II GRXs could increase abiotic stress tolerance in tomato by directly reducing ROS, deglutathionylation of target enzymes, or regulating gene expression through transcription factors (Wu et al., 2017).

REFERENCES

- Alam, B. & Jacob J. (2002). Overproduction of photosynthetic electrons is associated with chilling injury in green leaves. *Photosynthetica*, 40, 91-95.
- Balk, J., & Pilon, M. (2011). Ancient and essential: the assembly of iron–sulfur clusters in plants. *Trends in plant science*, 16, 218-226.
- Burney, J., & Ramanathan, V. (2014). Recent climate and air pollution impact on Indian agriculture. *Proceedings of the National Academy of Sciences*, 111(46), 16319-16324.
- Camejo, D., Rodríguez, P., Morales, M.A., Dell’Amico, J.M., Torrecillas, A. & Alarcón, J.J. (2005). High temperature effects on photosynthetic activity of two tomato cultivars with different heat susceptibility. *Journal of plant physiology*, 162(3), 281-289.
- Charles, S. P., Silberstein, R., Teng, J., Fu, G., Hodgson, G., Gabrovsek, C., & Bathols, J. M. (2010). Climate analyses for south-west Western Australia. A report to the Australian government from the CSIRO south-west Western Australia sustainable yields project. *Details Published by CSIRO© 2010 all rights reserved. This work is copyright. Apart from any use as permitted under the Copyright Act 1968, no part may be reproduced by any process without prior written permission from CSIRO. ISSN.*
- Cheng, N.H., Liu, J.Z., Brock, A., Nelson, R.S. & Hirschi, K.D. (2006). AtGRXcp, an Arabidopsis chloroplastic glutaredoxin, is critical for protection against protein oxidative damage. *Journal of Biological Chemistry*, 281, 26280-26288.
- Cheng, N. H., Liu, J. Z., Liu, X., Wu, Q., Thompson, S. M., Lin, J., ... & Hirschi, K. D. (2011). Arabidopsis monothiol glutaredoxin, *AtGRXS17*, is critical for temperature-dependent

- postembryonic growth and development via modulating auxin response. *Journal of Biological Chemistry*, 286(23), 20398-20406.
- Das, P., Samantaray, S., & Rout, G. R. (1997). Studies on cadmium toxicity in plants: a review. *Environmental pollution*, 98(1), 29-36.
- Dos Santos, C. V., & Rey, P. (2006). Plant thioredoxins are key actors in the oxidative stress response. *Trends in plant science*, 11(7), 329-334.
- Duan, M., Ma, N.N., Li, D., Deng, Y.S., Kong, F.Y., Lv, W. and Meng, Q.W. (2012). Antisense-mediated suppression of tomato thylakoidal ascorbate peroxidase influences anti-oxidant network during chilling stress. *Plant physiology and biochemistry*, 58, 37-45.
- FAO (Food and Agriculture Organization of the United Nations). (2017). *FAOSTAT Database*. <http://faostat3.fao.org/>.
- Foy, C. D., Chaney, R. T., & White, M. C. (1978). The physiology of metal toxicity in plants. *Annual review of plant physiology*, 29(1), 511-566.
- Foyer, C.H., & Noctor, G. (2005.) Redox homeostasis and antioxidant signaling: a metabolic interface between stress perception and physiological responses. *The Plant Cell*, 17, 1866-1875.
- Garg, R., Jhanwar, S., Tyagi, A. K., & Jain, M. (2010). Genome-wide survey and expression analysis suggest diverse roles of glutaredoxin gene family members during development and response to various stimuli in rice. *DNA research*, 17(6), 353-367.
- Gillet, S., Decottignies, P., Chardonnet, S., & Le Maréchal, P. (2006). Cadmium response and redoxin targets in *Chlamydomonas reinhardtii*: a proteomic approach. *Photosynthesis Research*, 89(2-3), 201-211.

- Hu, Y., Wu, Q., Sprague, S. A., Park, J., Oh, M., Rajashekar, C. B., & White, F. F. (2015). Tomato expressing Arabidopsis glutaredoxin gene *AtGRXS17* confers tolerance to chilling stress via modulating cold responsive components. *Horticulture research*, 2, 1-11.
- Hu, Y., Wu, Q., Peng, Z., Sprague, S.A., Wang, W., Park, J., Akhunov, E., Jagadish, K.S., Nakata, P.A., Cheng, N. and Hirschi, K.D. (2017). Silencing of *OsGRXS17* in rice improves drought stress tolerance by modulating ROS accumulation and stomatal closure. *Scientific reports*, 7(1), 1-14.
- Hussain, A.M. & Lunven, P. (1987). Urbanization and hunger in the cities. *Food and Nutrition Bulletin*, 9(4), 1-12.
- IBM Corp. Released 2017. IBM SPSS Statistics for Macintosh, Version 25.0. Armonk, NY: IBM Corp.
- Iñigo, S., Durand, A. N., Ritter, A., Le Gall, S., Termathe, M., Klassen, R., ... & Cammue, B. P. (2016). Glutaredoxin *GRXS17* associates with the cytosolic iron-sulfur cluster assembly pathway. *Plant physiology*, 172(2), 858-873.
- Jinek, M., Chylinski, K., Fonfara, I., Hauer, M., Doudna, J. A., & Charpentier, E. (2012). A programmable dual-RNA-guided DNA endonuclease in adaptive bacterial immunity. *science*, 337(6096), 816-821.
- Kang, B. C., Wu, Q., Sprague, S., Park, S., White, F. F., Bae, S. J., & Han, J. S. (2019). Ectopic overexpression of an Arabidopsis monothiol glutaredoxin *AtGRXS17* affects floral development and improves response to heat stress in chrysanthemum (*Chrysanthemum morifolium* Ramat.). *Environmental and Experimental Botany*, 167, 103864.

- Khan, N.A., & Singh, S. (2008). Abiotic stress and plant responses. IK International, New Delhi, pp.205-215.
- Kingston-Smith, A.H. and Foyer, C.H. (2000). Bundle sheath proteins are more sensitive to oxidative damage than those of the mesophyll in maize leaves exposed to paraquat or low temperatures. *Journal of Experimental Botany*, 51(342), 123-130.
- Knuesting, J., Riondet, C., Maria, C., Kruse, I., Bécuwe, N., König, N., ... & Gaymard, F. (2015). Arabidopsis glutaredoxin S17 and its partner, the nuclear factor Y subunit C11/negative cofactor 2 α , contribute to maintenance of the shoot apical meristem under long-day photoperiod. *Plant physiology*, 167(4), 1643-1658.
- Lemaire, S. D., Michelet, L., Zaffagnini, M., Massot, V., & Issakidis-Bourguet, E. (2007). Thioredoxins in chloroplasts. *Current genetics*, 51(6), 343-365.
- Li, S. (2014). Redox modulation matters: emerging functions for glutaredoxins in plant development and stress responses. *Plants*, 3(4), 559-582.
- Lukatkin, A.S., Brazaityte, A., Bobinas, C. and Duchovskis, P. (2012). Chilling injury in chilling-sensitive plants: a review. *Agriculture*, 99(2), 111-124.
- Mahajan, S., & Tuteja, N. (2005). Cold, salinity and drought stresses: an overview. *Archives of biochemistry and biophysics*, 444, 139-158.
- Method of the Year 2011. Nature Methods*. 9(1): 1. January 2012 doi:10.1038/nmeth.1852. PMID 22312634.
- Medici, L.O., Azevedo, R.A., Smith, R.J. and Lea, P.J. (2004). The influence of nitrogen supply on antioxidant enzymes in plant roots. *Functional Plant Biology*, 31, 1-9.

- Mittler, R. (2002). Oxidative stress, antioxidants and stress tolerance. *Trends in plant science*, 7, 405-410.
- Mittler, R., Vanderauwera, S., Gollery, M., & Van Breusegem, F. (2004). Reactive oxygen gene network of plants. *Trends in plant science*, 9(10), 490-498.
- Moseler, A., Aller, I., Wagner, S., Nietzel, T., Przybyla-Toscano, J., Mühlenhoff, U., ... & Meyer, A. J. (2015). The mitochondrial monothiol glutaredoxin *S15* is essential for iron-sulfur protein maturation in *Arabidopsis thaliana*. *Proceedings of the National Academy of Sciences*, 112(44), 13735-13740.
- Murashige, T., & Skoog, F. (1962). A revised medium for rapid growth and bio assays with tobacco tissue cultures. *Physiologia plantarum*, 15, 473-497.
- Park, S. H., Morris, J. L., Park, J. E., Hirschi, K. D., & Smith, R. H. (2003). Efficient and genotype-independent *Agrobacterium*-mediated tomato transformation.
- Rey, P., Becuwe, N., Tourrette, S., & Rouhier, N. (2017). Involvement of *Arabidopsis* glutaredoxin *S14* in the maintenance of chlorophyll content. *Plant, Cell & Environment*, 40(10), 2319-2332.
- Rouhier, N., Couturier, J., Johnson, M. K., & Jacquot, J. P. (2010). Glutaredoxins: roles in iron homeostasis. *Trends in biochemical sciences*, 35(1), 43-52.
- Schippers, J. H., Foyer, C. H., & van Dongen, J. T. (2016). Redox regulation in shoot growth, SAM maintenance and flowering. *Current opinion in plant biology*, 29, 121-128.
- Science News Staff* (17 December 2015). "Breakthrough of the Year: CRISPR makes the cut".
- Smil, V. (2005). *Energy at the crossroads: global perspectives and uncertainties*. MIT press.

- Smiri, M., Chaoui, A., Rouhier, N., Gelhaye, E., Jacquot, J. P., & El Ferjani, E. (2011). Cadmium affects the glutathione/glutaredoxin system in germinating pea seeds. *Biological trace element research*, *142*(1), 93-105.
- Ströher, E., Grassl, J., Carrie, C., Fenske, R., Whelan, J., & Millar, A. H. (2016). Glutaredoxin S15 is involved in Fe-S cluster transfer in mitochondria influencing lipoic acid-dependent enzymes, plant growth, and arsenic tolerance in Arabidopsis. *Plant physiology*, *170*(3), 1284-1299.
- Sundaram, S. and Rathinasabapathi, B., 2010. Transgenic expression of fern *Pteris vittata* glutaredoxin PvGrx5 in Arabidopsis thaliana increases plant tolerance to high temperature stress and reduces oxidative damage to proteins. *Planta*, *231*, 361.
- Sundaram, S., Rathinasabapathi, B., Ma, L. Q., & Rosen, B. P. (2008). An arsenate-activated glutaredoxin from the arsenic hyperaccumulator fern *Pteris vittata* L. regulates intracellular arsenite. *Journal of Biological Chemistry*, *283*, 6095-6101.
- Sundaram, S., Wu, S., Ma, L. Q., & Rathinasabapathi, B. (2009). Expression of a *Pteris vittata* glutaredoxin PvGRX5 in transgenic *Arabidopsis thaliana* increases plant arsenic tolerance and decreases arsenic accumulation in the leaves. *Plant, cell & environment*, *32*, 851-858.
- Tester, M., & Langridge, P. (2010). Breeding technologies to increase crop production in a changing world. *Science*, *327*(5967), 818-822.
- Tomato Genome Consortium (2012). The tomato genome sequence provides insights into fleshy fruit evolution. *Nature*, *485*(7400), 635.

- Vido, K., Spector, D., Lagniel, G., Lopez, S., Toledano, M. B., & Labarre, J. (2001). A proteome analysis of the cadmium response in *Saccharomyces cerevisiae*. *Journal of Biological Chemistry*, 276(11), 8469-8474.
- Wahid, A., Gelani, S., Ashraf, M. and Foolad, M.R. (2007). Heat tolerance in plants: an overview. *Environmental and experimental botany*, 61(3), 199-223.
- Wang, K.R. (2002). Tolerance of cultivated plants to cadmium and their utilization in polluted farmland soils. *Acta Biotechnologica*, 22, 189-198.
- Wu, Q., Hu, Y., Sprague, S.A., Kakeshpour, T., Park, J., Nakata, P.A., Cheng, N., Hirschi, K.D., White, F.F. and Park, S. (2017). Expression of a monothiol glutaredoxin, *AtGRXS17*, in tomato (*Solanum lycopersicum*) enhances drought tolerance. *Biochemical and biophysical research communications*, 491(4), 1034-1039.
- Wu, Q., Lin, J., Liu, J. Z., Wang, X., Lim, W., Oh, M., ... & Hirschi, K. D. (2012). Ectopic expression of Arabidopsis glutaredoxin *AtGRXS17* enhances thermotolerance in tomato. *Plant biotechnology journal*, 10(8), 945-955.
- Wu, Q., Yang, J., Cheng, N., Hirschi, K.D., White, F.F. and Park, S. (2017). Glutaredoxins in plant development, abiotic stress response, and iron homeostasis: From model organisms to crops. *Environmental and Experimental Botany*, 139, 91-98.
- Xia, X. J., Fang, P. P., Guo, X., Qian, X. J., Zhou, J., Shi, K., ... & Yu, J. Q. (2018). Brassinosteroid-mediated apoplastic H₂O₂-glutaredoxin 12/14 cascade regulates antioxidant capacity in response to chilling in tomato. *Plant, cell & environment*, 41(5), 1052-1064.
- Yadav, S. S., Redden, R. J., Hatfield, J. L., Ebert, A. W., & Hunter, D. (Eds.). (2019). *Food Security and Climate Change*. John Wiley & Sons.

- Yadav, S. S., Redden, R. J., Hatfield, J. L., Lotze-Campen, H., & Hall, A. J. (2011). *Crop adaptation to climate change*. John Wiley & Sons.
- Yang, X., & Ma, K. (2010). Characterization of a thioredoxin-thioredoxin reductase system from the hyperthermophilic bacterium *Thermotoga maritima*. *Journal of bacteriology*, 192(5), 1370-1376.
- Zaffagnini, M., Michelet, L., Massot, V., Trost, P., & Lemaire, S. D. (2008). Biochemical characterization of glutaredoxins from *Chlamydomonas reinhardtii* reveals the unique properties of a chloroplastic CGFS-type glutaredoxin. *Journal of Biological Chemistry*, 283(14), 8868-8876.
- Zsögön, A., Cermak, T., Voytas, D. and Peres, L.E.P., 2017. Genome editing as a tool to achieve the crop ideotype and de novo domestication of wild relatives: case study in tomato. *Plant Science*, 256, 120-130.

FIGURES

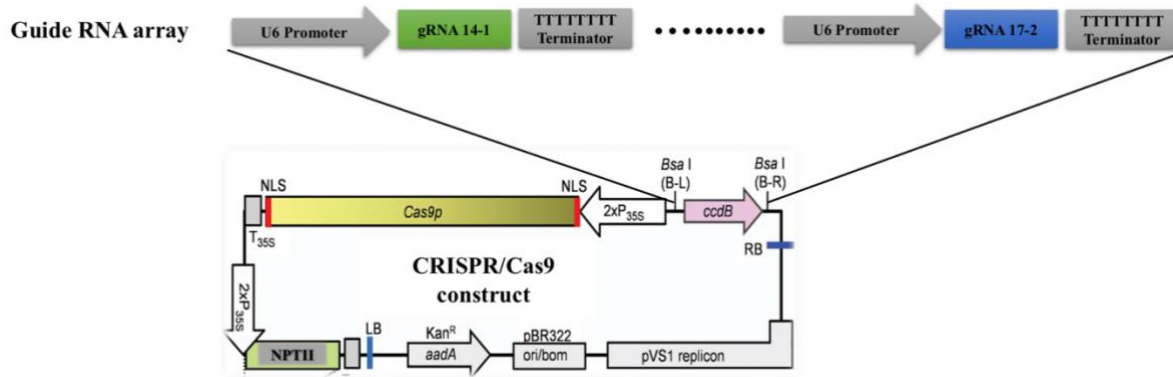


Figure 2-1 CRISPR/Cas9 binary vector harboring guide RNA array designed to target *S14*, *S15*, *S16* and *S17* glutaredoxins in tomato.

Maps of pYLCRISPR/Cas9P35S-N binary vector and guide RNA array inserted into the binary vector. BsaI cloning sites were used to insert gRNA array after restriction digestion.

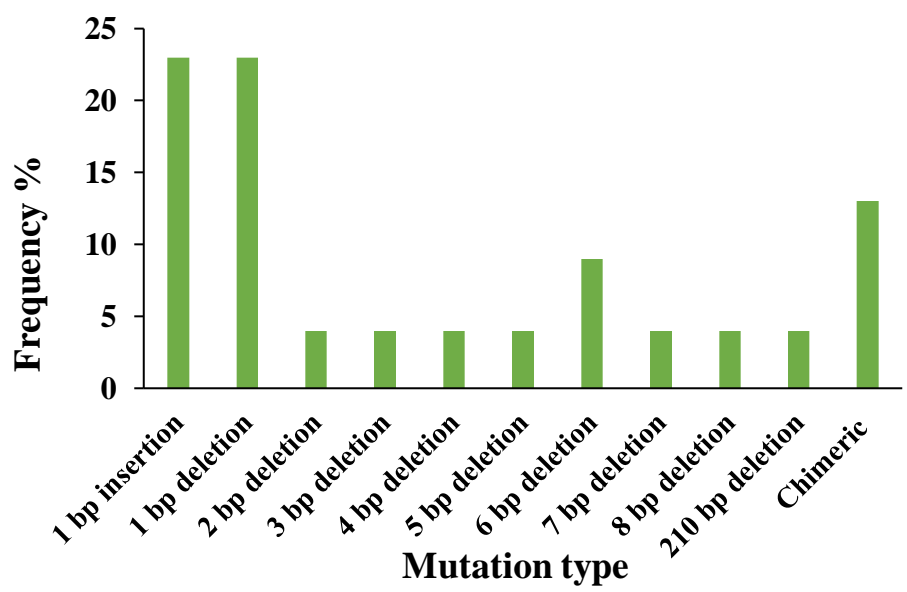
LB: Left border; NPTII: Neomycin phosphotransferase; p35S: Cauliflower mosaic virus 35S promoter; t35S: Cauliflower mosaic virus 35S terminator; NLS; Nuclear localization signal; RB: Right border.

a

SIGRXS14_g2	GTTGTTTCATGAAGGGGACCA AGG (WT)	SIGRXS16_g1	CGAGCGTACCACCGCTACC ACC (WT)
Line_1	GTTGTTTCATGAAGGGG A ACCA AGG (+1)	Line_1	CGAGCGTACCACCG...ACC ACC (-3)
Line_3	GTTGTTTCATGAAGGG..CCA AGG (-2)	Line_3	CGAGCGTACCACC..... ACC (-7)
Line_10	GTTGTTTCATGAAGGGG.CCA AGG (-1)	Line_10	CGAGCGTACCACCGCT.ACC ACC (-1)
Line_11	GTTGTTTCATGAAGGGNNNNNN (chimeric)	Line_11	CGAGCGTACGAGCGT.ACC ACC (-1)

SIGRXS15_g2	GTGCCAGACCTGCCTCGTT TGG (WT)	SIGRXS16_g2	GAACCGCCTTA ACTGAATCTTGG (WT)
Line_1	GTGCCAGACCTGCCTC.. TGTGG (-2)	Line_2	GAACCGCCTT..... AATCTTGG (-5)
Line_2a	GTGCCAGAC..... TGTGG (-8)	Line_9	GAACCGCCTT..... ATCTTGG (-6)
Line_2b	GTGCCAGACCTGCCTCG. TGTGG (-1)		
Line_3	GTGCCAGACCTGCCTCG TTTGTGG (+1)	SIGRXS17_g1	GATTGTCGCCGACGGATC ACCGG (WT)
Line_9	GTGCCAGACCTGC... TGTGG (-4)	Line_3	GATTGTCGCCGACGGAT CACCGG (+1)
Line_10	GTGCCAGACCTGCCTCG TTTGTGG (+1)		
Line_11	GTGCCAGACCTGCCTCGNNNNNN (chimeric)	SIGRXS17_g2	GCTAGCCTAGGAATGGCT GCAAGG (WT)
		Line_1	GCTAGCCTAGGAANNNNNNN (chimeric)
		Line_2	GCTAGCCTAGG..... TGCAGG (-6)
		Line_3	GCTAGCCTAGGAATGGC CTGCAGG (+1)

b



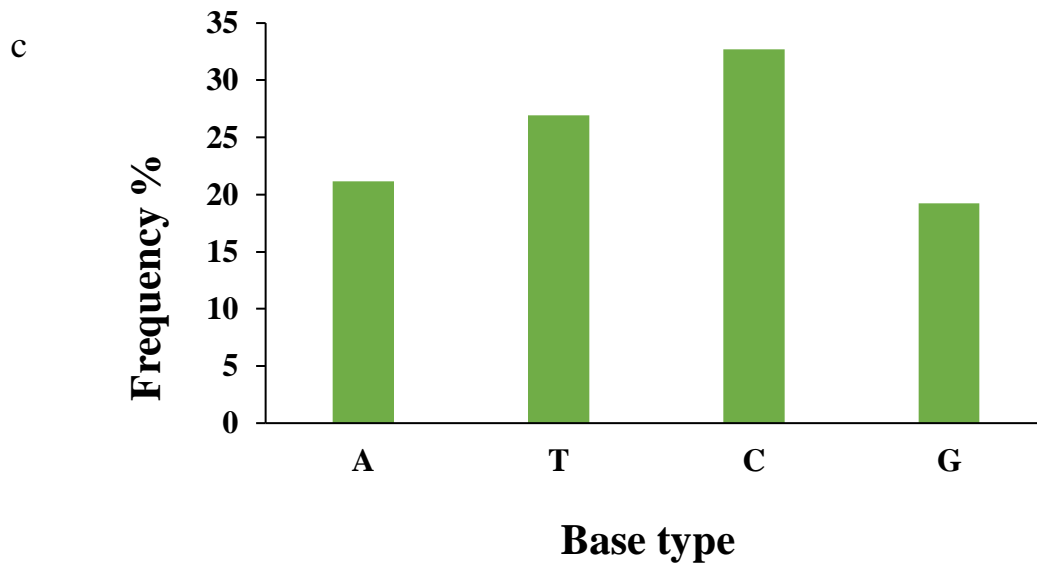


Figure 2-2 Genotyping analysis of CRISPR/Cas9-induced mutations in T0 transgenic tomato plants.

- (a) detection of targeted insertions and deletions at target sites based on DNA sequencing analysis.
 (b) Type and frequency of T0 mutations created using CRISPR/Cas9 system. (c) Frequency of each base insertions and deletions.



Figure 2-3 Phenotypic analysis of *s14*, *s16*, *s17* single, *s14::16* double, and *s14::16::17* triple mutant tomato lines in response to heat stress.

(a) Phenotypes of wild-type and *s14*, *s16*, *s17* single, *s14::16* double, and *s14::16::17* triple mutants grown under the normal condition at 24/20 °C day and night temperatures before heat treatment. (b) Phenotypes of wild-type and *s14*, *s16*, *s17*, *s14::16*, and *s14::16::17* mutants subjected to 38/28 °C, continued by 45/35 °C day and night temperatures for 10 days.

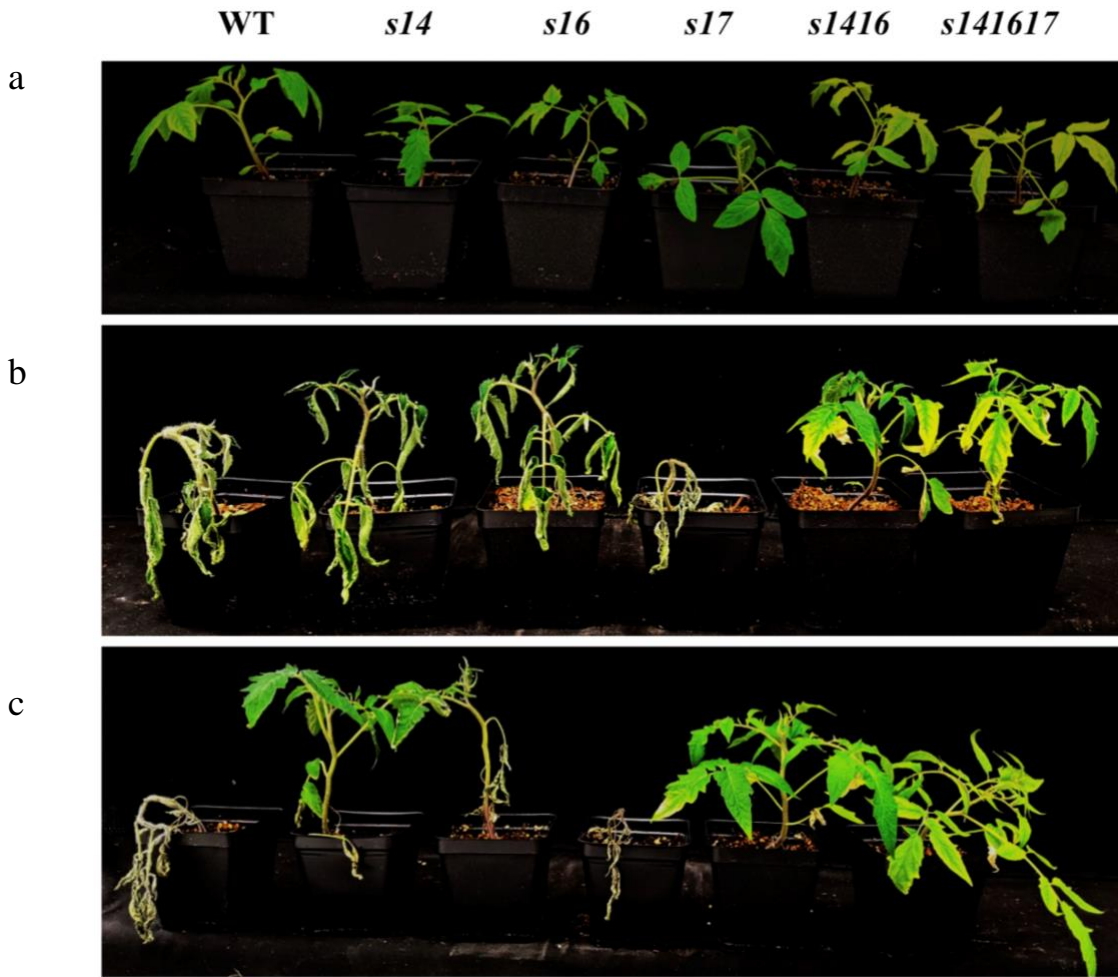


Figure 2-4 Phenotypic analysis of *s14*, *s16*, *s17* single, *s14::16* double and *s14::16::17* triple mutant tomato lines in response to drought stress.

(a) Phenotypes of wild-type and *s14*, *s16*, *s17* single, *s14::16* double, and *s14::16::17* triple mutants grown under control condition with regular watering before drought treatment. (b) Phenotypes of wild-type and *s14*, *s16*, *s17*, *s14::16*, and *s14::16::17* mutants subjected to drought stress by withholding water for 15 days. (c) Phenotypes of wild-type and *s14*, *s16*, *s17* single, *s14::16* double and *s14::16::17* triple mutants after one week of recovery under control condition with regular watering.

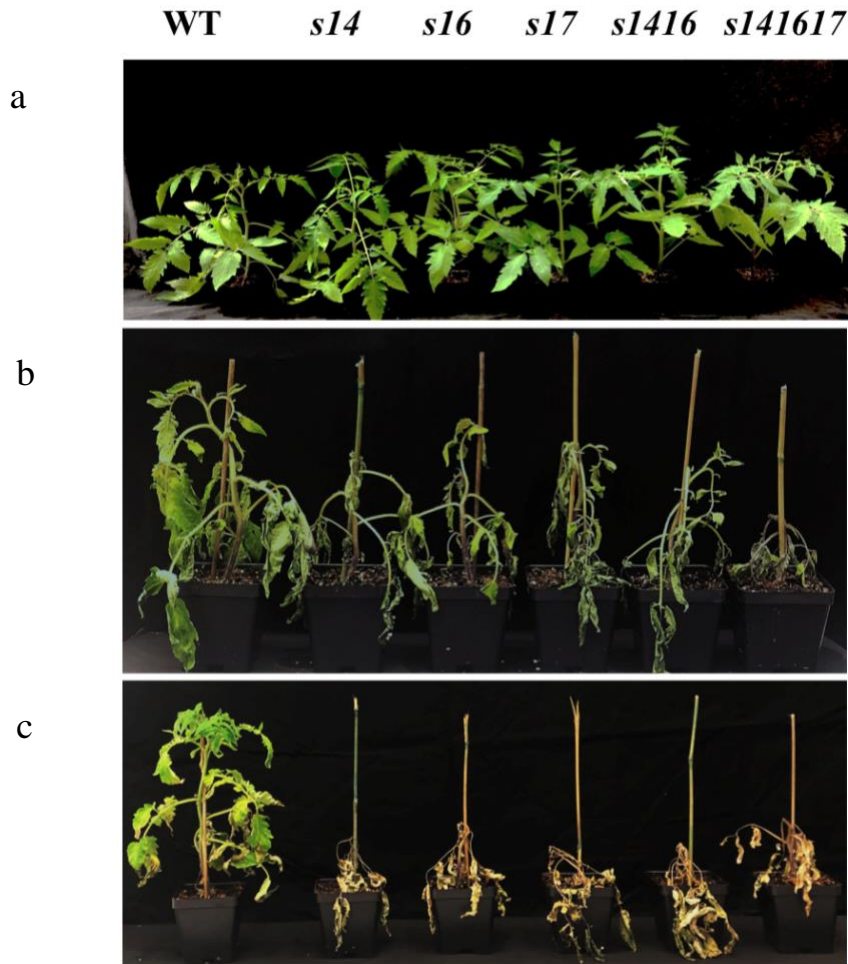
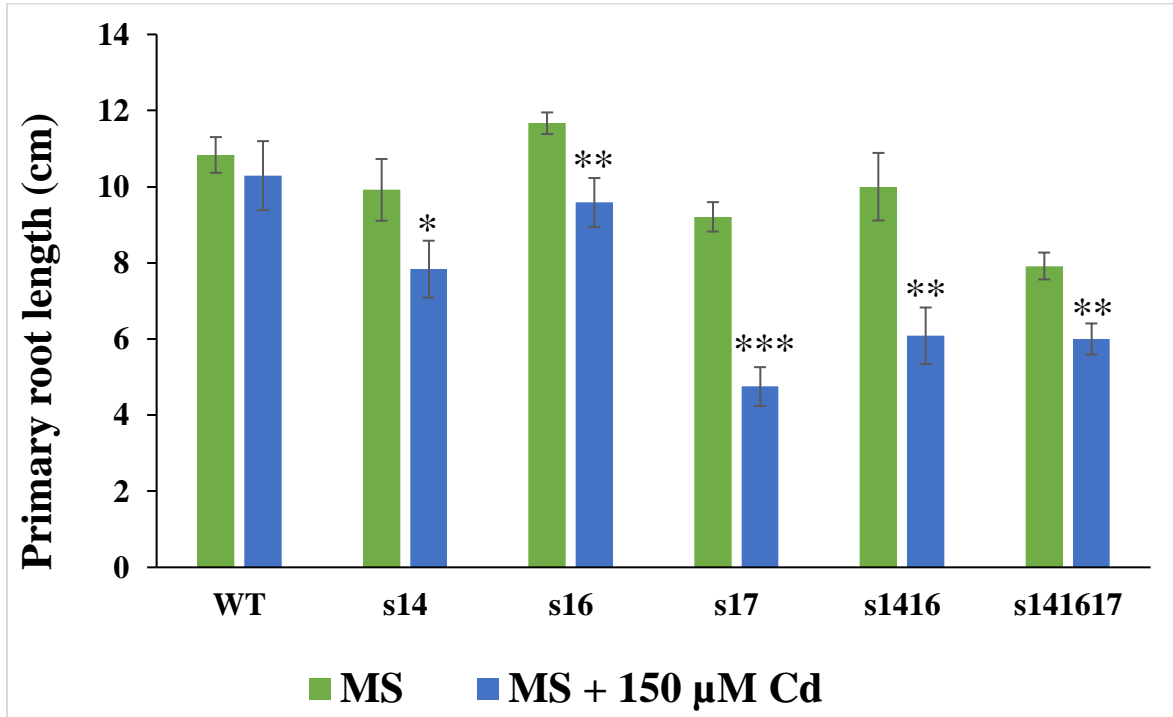


Figure 2-5 Phenotypic analysis of *s14*, *s16*, *s17* single, *s14::16* double, and *s14::16::17* triple mutant tomato lines in response to chilling stress.

(a) Phenotypes of wild-type and *s14*, *s16*, *s17* single, *s14::16* double, and *s14::16::17* triple mutants grown under control condition at 24/20 °C day and night temperatures before chilling treatment. (b) Phenotypes of wild-type and *s14*, *s16*, *s17*, *s14::16*, and *s14::16::17* mutants subjected to chilling stress at 4 °C for four weeks. (c) Phenotypes of wild-type and *s14*, *s16*, *s17* single, *s14::16* double and *s14::16::17* triple mutants after one week of recovery under the control condition at 24/20 °C day and night temperatures.

a



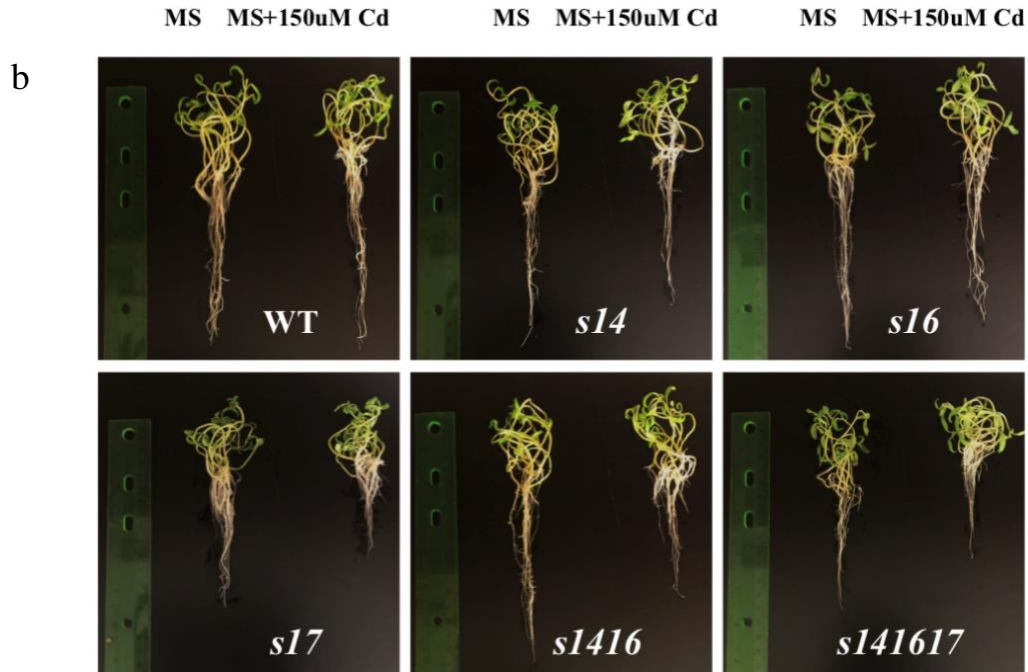


Figure 2-6 Phenotypic analysis of *s14*, *s16*, *s17* single, *s14::16* double, and *s14::16::17* triple mutant tomato lines in response to cadmium toxicity stress

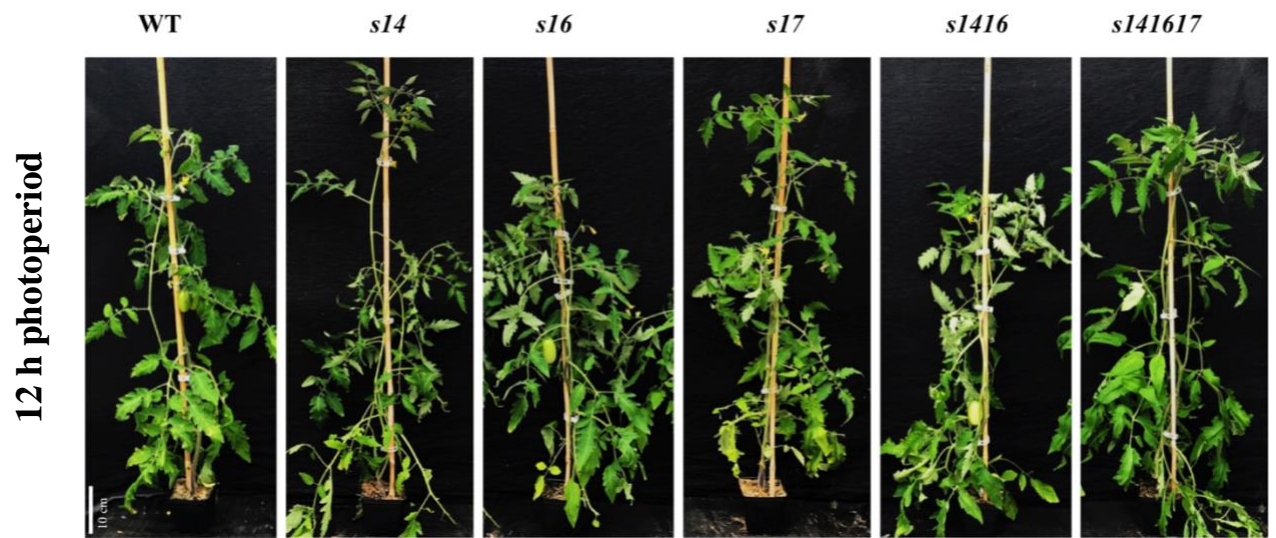
(a) Root length of wild-type and *s14*, *s16*, *s17* single mutants, *s14::16* double mutant, and *s14::16::17* triple mutant lines growing on MS media and 150 μ M cadmium containing MS media.

(b) The phenotype of wild-type and *s14*, *s16*, *s17* single mutants, *s14::16* double mutant, and *s14::16::17* triple mutant lines grown on MS media.

a



b



c

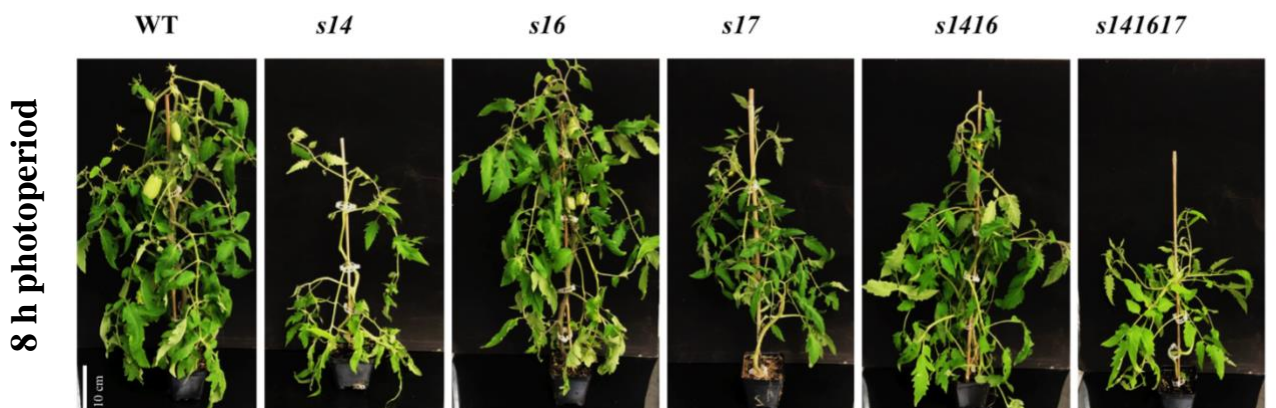


Figure 2-7 Phenotypic analysis of wild-type and mutant lines under different photoperiods in growth chambers.

- (a) Phenotype of wild-type and *s14::16::17* triple mutant under 8, 12, and 16 h photoperiods.
Phenotype of wild-type, *s14*, *s16*, *s17* single mutants, *s14::16* double mutants, and *s14::16::17* triple mutants under (b) 12 h photoperiod and, (c) 8 h photoperiod.

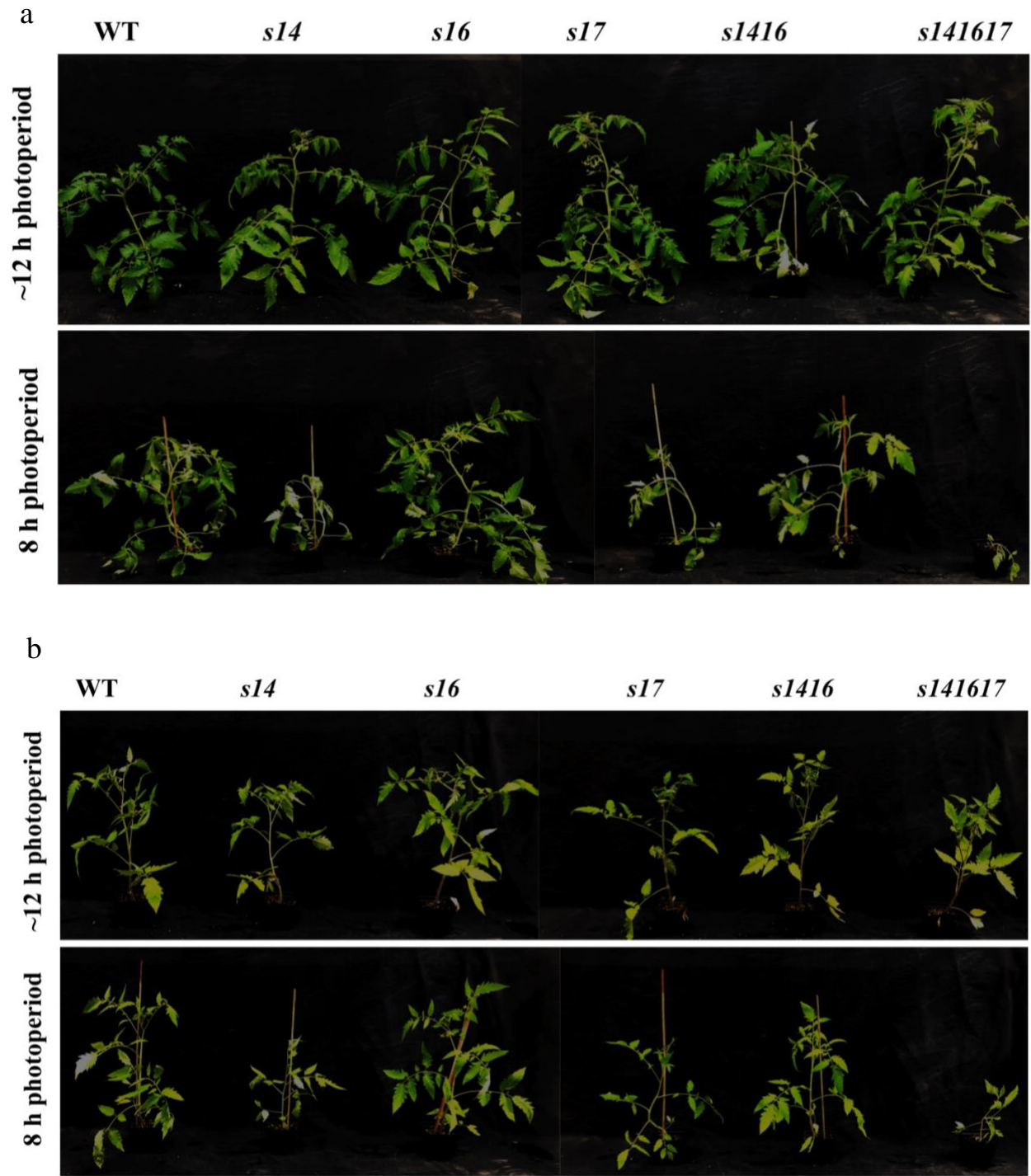


Figure 2-8 Phenotypic analysis of wild-type and mutant tomato lines under different levels of nutrients and photoperiods in greenhouse.

Phenotype of wild-type, *s14*, *s16*, *s17* single mutants, *s14::16* double mutants and *s14::16::17* triple mutants under 12 and 8 h photoperiods. (a) Tomato seedlings were regularly fertilized. (b) Tomato seedlings were not fertilized.

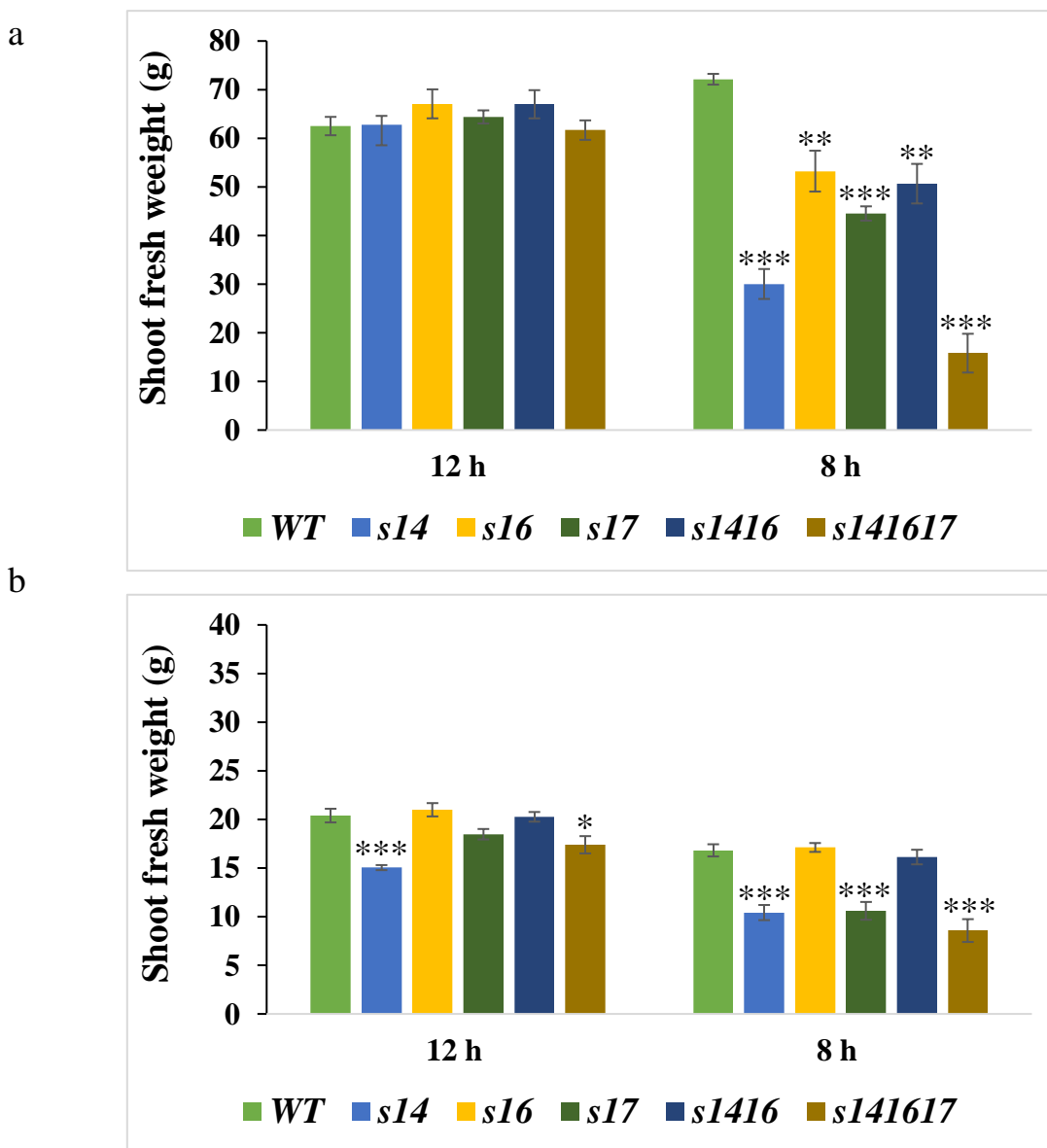


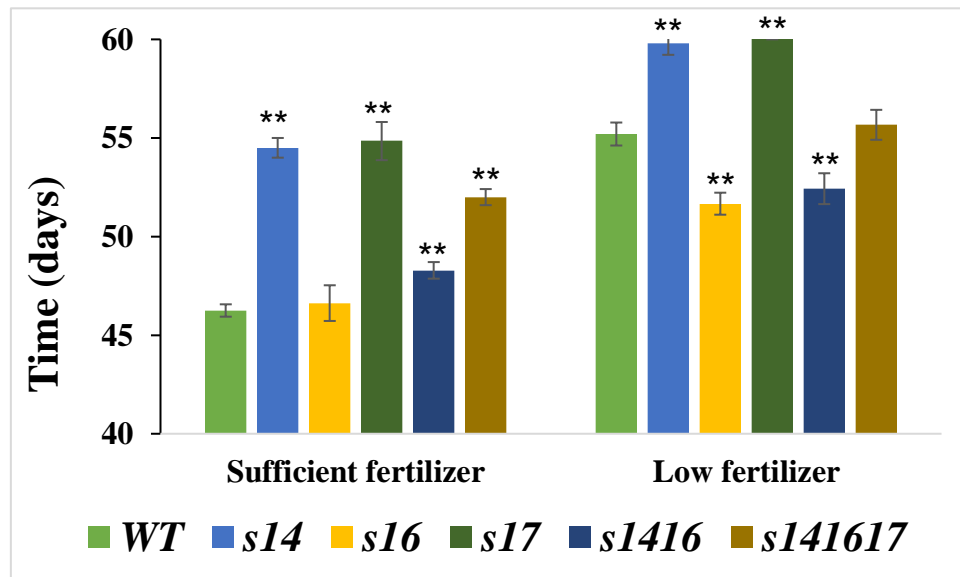
Figure 2-9 Shoot fresh weight of wild-type and mutant tomato lines under different levels of nutrients and photoperiods.

Shoot fresh weight of wild-type and *s14*, *s16*, *s17* single mutants, *s14::16* double mutant, and *s14::16::17* triple mutant lines under 12 h and 8 h photoperiods (a) with sufficient and (b) low fertilizer application. Error bars represent \pm SE of 8 replications. Student *t*-test, * p <0.05; ** p <0.01; *** p <0.001.

a



b



c



d



e



f

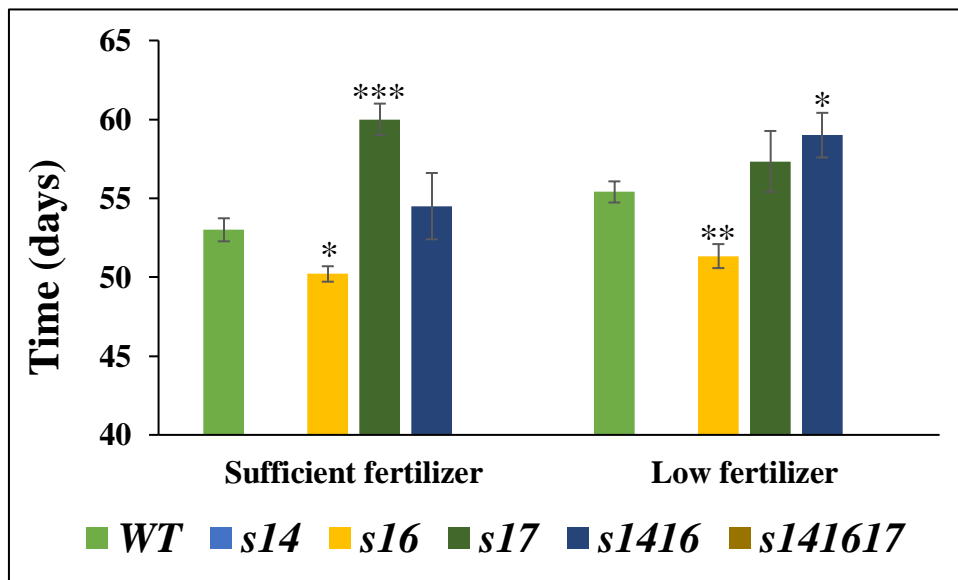


Figure 2-10 Flowering time of wild-type and mutant tomato lines under different levels of nutrients and photoperiods

(a) Flowers of wild-type and mutant lines under 12 h, and b) 8 h photoperiods with sufficient application of fertilizer. (c) Flowers of wild-type and mutant lines under 12 h, and (d) 8 h photoperiods with low application of fertilizer. (e) Flowering time of wild-type and mutant lines under 12 h and (f) 8 h photoperiods with sufficient and low fertilizer applications. Error bars represent \pm SE of 8 replications. Student *t*-test, * $p < 0.05$; ** $p < 0.01$; *** $p < 0.001$.

TABLES

Table 2-1 List of primers used for screening and genotyping CRISPR/Cas9 generated class II *Slgrxs* mutant lines.

Gene	Forward primer	Reverse primer
<i>S14-gRNA1</i>	5'-tcttgggagtaacgacaaagagta-3'	5'-agggatcttaaccgtccatccc-3'
<i>S14-gRNA2</i>	5'-tcccccaaccttatggctactc-3'	5'-acaacaatgtcacagccaccaa-3'
<i>S15-gRNA1&2</i>	5'-atgtgttagcccatagacagga-3'	5'-tctggcacttattggagcatctg-3'
<i>S16-gRNA1</i>	5'-tcattctcacacaacctgcca-3'	5'-agcatcaccaagacacatcctg-3'
<i>S16-gRNA2</i>	5'-tgcttagaatcccaactgcacc-3'	5'-caataaggtcctccaagggcac-3'
<i>S17-gRNA1</i>	5'-gaaatttcgtattgttctttgagggt-3'	5'-aatgggcatgtgggaaatcagt-3'
<i>S17-gRNA2</i>	5'-cctctgattgaacctacgttttgc-3'	5'-ccaagaagttcacccttcagt-3'
Kanamycin marker	5'-gaggctattcggctatgactg-3'	5'-atcgggagcggcgataccgta-3'
Cas9	5'-ccttactacgttgctcctcttg-3'	5'-gatagggagatgatcaggaga-3'

Table 2-2 T0 transgenic tomato lines generated using the CRISPR/Cas9 system.

Target genes	<i>GRXS14</i>		<i>GRXS15</i>		<i>GRXS16</i>		<i>GRXS17</i>		KAN	Cas9
Line #	gRNA1	gRNA2	gRNA1	gRNA2	gRNA1	gRNA2	gRNA1	gRNA2		
1	-/-	+/-	-/-	+/-	+/-	-/-	-/-	c	+	+
*2	-/-	-/-	-/-	+/-	-/-	+/-	-/-	+/-	+	+
*3	-/-	+/-	-/-	+/-	+/-	-/-	+/-	+/-	+	+
7	-/-	-/-	-/-	-/-	-/-	-/-	-/-	-/-	+	+
9	-/-	-/-	-/-	+/-	-/-	+/-	-/-	-/-	+	+
*10	-/-	+/-	-/-	+/-	+/-	-/-	-/-	-/-	+	+
11	-/-	c	-/-	c	+/-	-/-	-/-	-/-	+	+
12	-/-	-/-	-/-	-/-	-/-	-/-	-/-	-/-	+	+
15	-/-	-/-	-/-	-/-	-/-	-/-	-/-	-/-	+	+
16	-/-	-/-	-/-	-/-	-/-	-/-	-/-	-/-	+	+

Note, C chimeric mutation; +/- heterozygous mutation; -/- null; *Selected lines for further analysis

Table 2-3 Guide RNA efficiency in Agrobacterium-mediated gene transformation of tomato.

gRNA	Mutation efficiency (%)	Guide RNA + PAM	Target gene
g14-1	0	GGCAACTCCCCTCCGTTATC AGG	<i>GRXS14</i>
g14-2	20	GTTGTTTCATGAAGGGGACCA AGG	<i>GRXS14</i>
g15-1	0	GAACTCTCAAGCTTACTAGT AGG	<i>GRXS15</i>
g15-2	30	GTGCCAGACCTGCCTCGTTGT TGG	<i>GRXS15</i>
g16-1	20	GCTCGCATGGTGGCGAGTGGT TGG	<i>GRXS16</i>
g16-2	10	GAACCGCCTTAACTGAATCT TGG	<i>GRXS16</i>
g17-1	5	GATTGTGCGCCGACGGATC CCGG	<i>GRXS17</i>
g17-2	15	GCTAGCCTAGGAATGGCTGC AGG	<i>GRXS17</i>
Average	12.5		

Table 2-4 Detected genotype of T1 Transgenic tomato lines segregated from CRISPR/Cas9 generated T0 parents.

Line #2	<i>GRXS15</i>	<i>GRXS16</i>	<i>GRXS17</i>	KAN	Cas9
*1	-/-	+/-	+/+	-	-
2	-/-	+/-	-/-	-	-
3	-/-	+/-	-/-	-	-
4	-/-	+/-	-/-	-	-
5-50	×	×	×	+	+

Line #3	<i>GRXS14</i>	<i>GRXS15</i>	<i>GRXS16</i>	<i>GRXS17</i>	KAN	Cas9
1	-/-	+/-	+/-	+/-	-	-
2	+/-	+/-	-/-	+/-	-	-
3	+/-	-/-	+/-	+/-	-	-
4	+/-	-/-	+/-	+/-	-	-
5	+/+	+/-	+/-	+/-	-	-
6	+/+	-/-	+/-	+/-	-	-
7	+/+	-/-	+/-	+/-	-	-
8	-/-	-/-	+/-	-/-	-	-
*9	+/+	+/-	+/+	+/+	-	-
10	+/-	-/-	+/+	+/-	-	-
11-50	×	×	×	×	+	+

Line #10	<i>GRXS14</i>	<i>GRXS15</i>	<i>GRXS16</i>	KAN	Cas9
1	+/+	-/-	+/-	-	-
2	+/+	+/-	-/-	-	-
*3	+/-	-/-	+/+	-	-
*4	+/-	+/-	-/-	-	-
5	+/-	+/-	-/-	-	-
6	+/-	-/-	-/-	-	-
7-50	×	×	×	+	+

Note, +/- heterozygous mutation; ++ homozygous mutation; -/- null; × were not genotyped; * Selected lines for further analysis

Table 2-5 Detected genotype of T2 transgenic tomato lines segregated from T1 CRISPR/Cas9 mutated lines.

T1 plants	Genes	Edits	T2 plants	Genes	Edits	# of plants genotyped	# of plants with edits	Summary of mutated genes
2-1	<i>grxs16</i> <i>grxs 17</i>	+/- +/+	2-1 -1	<i>grxs 17</i>	+/+	11	11	* <i>grxs 17</i>
3-9	<i>grxs 14</i> <i>grxs 15</i> <i>grxs 16</i> <i>grxs 17</i>	+/+ +/- +/+ +/+	3-9-1	<i>grxs 14</i> <i>grxs 16</i> <i>grxs 17</i>	+/+ +/+ +/+	14	7	* <i>grxs 141617</i>
			3-9-2	<i>grxs 14</i> <i>grxs 15</i> <i>grxs 16</i> <i>grxs 17</i>	+/+ +/- +/+ +/+	14	7	<i>grxs 14151617</i>
10-3	<i>grxs 14</i> <i>grxs S16</i>	+/- +/+	10-3-1	<i>grxs 14</i> <i>grxs 16</i>	+/+ +/+	9	2	* <i>grxs 1416</i>
			10-3-2	<i>grxs 14</i> <i>grxs 16</i>	+/- +/+	9	5	<i>grxs 1416</i>
			10-3-3	<i>grxs 16</i>	+/+	9	2	* <i>grxs 16</i>
10-4	<i>grxs 14</i> <i>grxs 15</i>	+/- +/-	10-4-1	<i>grxs 14</i>	+/+	23	5	* <i>grxs 14</i>
			10-4-2	<i>grxs 14</i>	+/-	23	6	<i>grxs 14</i>
			10-4-3	<i>grxs 14</i> <i>grxs 15</i>	+/+ +/-	23	2	<i>grxs 1415</i>
			10-4-4	<i>grxs 14</i> <i>grxs 15</i>	+/- +/-	23	7	<i>grxs 1415</i>
			10-4-5	-	Null	23	3	Null

Note, +/- heterozygous mutation; +/+ homozygous mutation; * Selected homozygous mutant plants for further experiments.

Table 2-6 Three-way ANOVA for shoot fresh weight in wild-type and *s14*, *s16*, *s17*, *s14::16*, and *s14::16::17* mutant lines.

Source	Type III Sum of Squares	df	Mean Square	F	Sig.
Corrected Model	72033.217 ^a	23	3131.879	104.889	.000
Intercept	169768.344	1	169768.344	5685.661	.000
Fertilizer	50528.161	1	50528.161	1692.224	.000
Photoperiod	5378.193	1	5378.193	180.119	.000
Genotype	4863.484	5	972.697	32.576	.000
Nutrient* Photoperiod	1623.864	1	1623.864	54.384	.000
Nutrient* Genotype	1839.803	5	367.961	12.323	.000
Photoperiod* Genotype	3006.676	5	601.335	20.139	.000
Nutrient* Photoperiod* Genotype	2228.874	5	445.775	14.929	.000
Error	3553.225	119	29.859		
Total	242888.741	143			

Note, ^a R Squared = 0.953 (Adjusted R Squared = 0.944)

Sig. < 0.05: statistically significant; Sig. < 0.001: statistically highly significant

Table 2-7 Three-way ANOVA for flowering time in wild-type and *s14*, *s16*, *s17*, *s14::16* and *s14::16::17* mutant lines.

Source	Type III Sum of Squares	df	Mean Square	F	Sig.
Corrected Model	1617.213 ^a	23	70.314	13.769	.000
Intercept	97385.442	1	97385.442	19070.856	.000
Fertilizer	316.064	6	52.677	10.316	.000
Photoperiod	56.287	1	56.287	11.023	.001
Genotype	637.364	5	127.473	24.963	.000
Nutrient* Photoperiod	101.104	1	101.104	19.799	.000
Nutrient* Genotype	18.874	4	4.718	.924	.454
Photoperiod* Genotype	129.071	3	43.024	8.425	.000
Nutrient* Photoperiod* Genotype	29.886	3	9.962	1.951	.127
Error	439.160	86	5.107		
Total	308191.000	110			

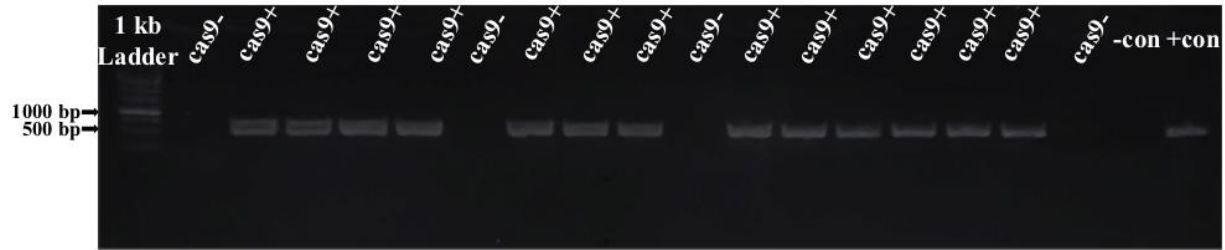
Note, ^a R Squared = 0.786 (Adjusted R Squared = 0.729)

Sig. < 0.05: statistically significant; Sig. < 0.001: statistically highly significant

Table 2-8 Summary of phenotyping analysis in wild-type and *s14*, *s16*, *s17*, *s14::16* and *s14::16::17* mutant lines.

Abiotic stress	# of stress treatments	# of replications/ genotype of each stress treatment	Total # of replications/ genotype	# of plants with detected phenotype/ genotype	% of plants with detected phenotype/ genotype
Heat	3	6	18	15	83.4
Chilling	3	6	18	18	100
Drought	2	3-6	9	7	77.8
Short photoperiod	5	6-8	32	27	84.4
Nutrient deficiency	1	8	8	8	100
Cadmium toxicity	3	6	18	15	83.4

SUPPLEMENTARY FIGURES



Supplementary Figure S 2-1 PCR analysis to screen for CRISPR/Cas9-free plants.

Positive control: Plasmid, negative control: wild-type tomato plants. Cas9 PCR was performed on 50 plants from each line using Cas9 specific primers listed in **Table 2-1**.

Chapter 3 - **Expression of mouse small interfering RNAs in lettuce using artificial microRNA technology**

*This paper was published in the Biotechniques Journal.

ABSTRACT

Artificial miRNA (amiRNA) technology has recently enabled the generation of small interfering RNAs (siRNAs) to regulate gene expression in organisms by either degrading target messenger RNA (mRNA) and/or by inhibiting protein translation. However, the application of siRNAs to alter gene expression is challenging predominantly due to the delivery and instability of siRNA into the host system. Thus, establishing a robust system to successfully deliver intact siRNAs is critical for the development of siRNA-based therapeutics. Here, we show that the siRNA targeted to animal mRNA can be heterologously expressed and produced in lettuce. We demonstrated that endogenous rice microRNA (miRNA) precursor, osa-MIR528, was customized to produce siRNAs targeting mRNA of mouse complement factor 7 (CF7) and complement component 3 (C3). miRNAs of cereals such as rice are among the most common plant miRNAs found in human blood. MIR168a, a rice-based miRNA is the first to be produced bioavailable and bioactive in animals. Making rice miRNA precursors ideal templates to design amiRNAs targeting animal mRNAs. Both CF7 and C3 proteins are involved in blood clotting which could lead to cardiovascular dysfunction. Expression of both primary and mature CF7 and C3 siRNAs in lettuce was validated by semi-quantitative real time-PCR and end-point PCR, respectively, and was confirmed via Sanger sequencing. Our study demonstrates an applicable tool to alter gene expression in the targeted host and has potential utility in siRNA-based oral therapeutics.

INTRODUCTION

RNA interference (RNAi) is a natural process by which small interfering RNA (siRNA) or microRNA (miRNA) molecules inhibit gene expression or translation by targeting messenger RNA molecules. siRNAs are 19–27-bp, double-stranded molecules that can be derived from double-stranded RNAs or hairpin RNA splicing. Exogenously introduced siRNAs can be used to knock down virtually any gene in host cells; hence, RNAi has proven to be a valuable technology for the functional analysis of genes (Bobbin et al., 2016; Voinnet et al., 1991). Development of therapeutic applications of RNAi in gene therapy to reduce the expression of disease-related proteins further highlights the importance of RNAi technology (Kedmi et al., 2018). Recent researches on therapeutic applications of RNAi such as gene therapy, drug production or reduced excessive expression of disease-related proteins have been very promising (Aagaard and Rossi, 2007; Higuchi et al., 2010). To date, siRNAs are used as an important agent in a therapeutic trial for several different diseases (Lares et al., 2010). Over the last couple of decades, several genes related to diseases such as cancer, heart disease, viral infection, and inflammatory diseases have been targeted by RNAi (Sioud, 2004; Hu et al., 2010; Cho et al., 2010; Kota et al., 2009). However, there are some obstacles to the application of siRNAs. One of the major obstacles is the fast degradation and instability of siRNA. Thus, many attempts such as lipid-based nanoparticles, cyclodextrin-containing polymer, ex vivo transfection, and siLL system have been utilized to achieve an efficient delivery system that also prevents siRNAs degradation (Tatiparti et al., 2017). Based on recent studies siRNAs ingested from a plant-based diet are bioactive and bioavailable suggesting that plants can be used as an intermediate organism to express and deliver siRNAs into target cells (Petrick et al., 2013; Tatiparti et al., 2017). Moreover, plant-based siRNAs are more stable than synthetic siRNAs (Yang et al., 2016; Yang et al., 2018). Meanwhile, siRNAs from

other organisms are found in human fluids probably through diet suggesting siRNA transfer between organisms is natural and possible (Wang et al., 2012). Plants have been used as a valuable source to treat various diseases for thousands of years worldwide (Petrovska, 2012). However, using recombinant DNA technologies to produce plant-based remedies is new. Genetically modified plants can produce bio drugs that are healthier and cheaper than those made through animal cell culture or chemically synthesized (Schillberg et al., 1999). Not only cross kingdom miRNA has great potentials as a treatment for human or animal diseases, but also it can be used to study insect-plant interactions and protect plants against insect diseases by expressing siRNAs targeting disease-causing genes. Several studies have shown transgenic plants expressing dsRNAs, affected insects' targeted gene through RNAi.

Here, lettuce, *Lactuca sativa* L. was used as the intermediate organism to produce two siRNA molecules targeting mouse *C3* and *CF7* of the complement system. Lettuce was selected as host to produce mouse siRNAs because as a leafy plant has high biomass but unlike tobacco does not contain toxic phenolic and alkaloid compounds, therefore can be used for dietary siRNA delivery. Moreover, lettuce has a rapid life cycle and can be cultivated in indoor spaces (Fischer et al., 2004; Kanamoto et al., 2006). The mammalian complement system plays an important role in adaptive and innate immunity. *C3* is a 187 KDa protein with 1641 residues and is essential for the three complement activation pathways in mammals. *C3* has 13 domains, interacts with different proteins, and can function accordingly through conformational changes created by enzymatic cleavages (Janssen et al., 2005). *CF7* is a 93 KDa protein with 843 residues and is involved in membrane attack complex (MAC). Through binding to MAC, *CF7* undergoes configuration changes and acquires a hydrophobic site that enables *CF7* to attach to the membrane of pathogens like an anchor, causing cell lysis and death in pathogens (DiScipio et al., 1988).

Excessive production of members of mammalian complement system such as C3 and CF7 has shown to cause blood clotting, despite their important roles in adaptive and innate immunity system. Blood clotting or coagulation is a vital mechanism that stops bleeding after an injury in blood vessels. However, sometimes blood clotting happens in arteries and veins and does not dissolve naturally causing serious problems in the body's cardiovascular system (Rivard et al., 2005). Each year 300,000-600,000 persons in the U.S. are affected by blood clotting related diseases such as venous thromboembolism (VTE) (Beckman et al., 2010). There are different types of medications to interrupt blood clotting cascades, such as blood clot filter (Simon, 1984), anti-platelets, and anti-coagulation drugs. However, despite massive attempts to reduce deaths caused by blood clotting, there is still a high number of mortalities, which shows the imperfection of traditional therapeutic strategies. In such a situation, emerging roles of siRNAs in treating various diseases open an unconventional therapeutic path.

We hypothesized that *C3* and *CF7* siRNA vectors would be successfully integrated into the genome of lettuce and transcribed to form primary hairpin amiRNAs. Since, hairpin miRNA structures are natural targets of Dicer, the transcribed amiRNAs would also be targeted and chopped by Dicer to generate mature 20 nt *C3* and *CF7* siRNAs. Based on the expected size of primary and mature siRNAs, PCR technologies and Sanger sequencing will be used to detect and confirm the production of siRNAs in transgenic lettuce.

MATERIALS AND METHODS

Plasmid construction

To replace 21 bp of osa-MIR528 with target siRNAs (**Figure 3-1a**), three pairs of primers were designed. Primer sequences are shown in **Supplementary Table 3-1**. Sequences of target siRNAs were added to the PCR primers, so that amplified PCR products contain target siRNA sequences. Osa-MIR528 backbone was used as a template for PCR. The first PCRs using designed primer sets resulted in three DNA fragments containing target siRNAs. Finally, fusion PCR on the three PCR products produced one DNA fragment for subsequent cloning (**Supplementary Figure 3-1**). C3 and CF7 amiRNA fragments were then inserted into plant expression vector pBICaMV under the control of cauliflower mosaic virus (CaMV) 35S constitutive promoter and NOS (nopaline synthase) terminator (**Figure 3-1b**). Plant expression vectors harboring amiRNAs were then transformed into Top 10 *E. coli* chemical competent cells and the transformation was confirmed by both antibiotic selection and the PCR. Vectors were transformed into *Agrobacterium tumefaciens* strain LBA4404 using the freeze-thaw method (Holsters et al., 1978) and confirmed by both antibiotic selection and PCR. Each construct (C3 amiRNA, CF7 amiRNA, pBICaMV, and osa-MiR528) was transformed into *Lactuca sativa* L. var. Simpson using *Agrobacterium*-mediated transformation.

Plant material, transformation and growth condition

Leaf disc explants of lettuce (*Lactuca sativa* L. var. Simpson) were transformed using *Agrobacterium*-mediated transformation (Park et al., 2009). Surface sterilized seeds were germinated on MS inorganic salt medium (Murashige and skoog, 1962) containing 30 gL⁻¹ sucrose, pH 5.7, and 8 gL⁻¹ agar (PhytoTechnology, Shawnee Mission, KS, US). Six weeks old *in vivo* grown lettuce leaves were excised and precultured on MS inorganic salts with 100 mgL⁻¹ inositol,

MS vitamins, 30 gL⁻¹ sucrose, 2 mgL⁻¹ N-6(2-isopentenyl)-adenine, 0.1 mgL⁻¹ indoles acetic acid and 8 gL⁻¹ Agar for one day. Then, leaves were inoculated with *Agrobacterium* for 1 minute and re-cultured on the same medium for three days. Leaf sections were afterward transferred on selection medium with MS inorganic salts, 30 gL⁻¹ sucrose, 100 mgL⁻¹ inositol, MS vitamins, 0.4 mgL⁻¹ 6-benzyl-aminopurine, 0.05 mgL⁻¹ naphthaleneacetic acid, 100 mgL⁻¹ kanamycin, 250 mgL⁻¹ Clavamox® and 8 gL⁻¹ Agar. Cultures were kept at 22 °C and 14-h photoperiod for six to eight weeks to regenerate shoots, then were transferred to rooting medium for another six weeks. Lettuce seedlings were afterward established in soil and moved in growth chambers with 16-18 °C and 14-h photoperiod. Every week they were watered with Miracle-GroR for tomato (Scotts Miracle-Gro Products, Port Washington, NY, USA).

DNA isolation and screening for putatively transformed plants

Leaf tissue was collected from 4 weeks old wild-type and transgenic lettuce plants that were grown under controlled conditions. Total genomic DNA was isolated using 2% cetyltrimethylammonium bromide (CTAB). In addition to kanamycin screening, T1 plants were also genotyped using specific forward and reverse primers that were designed based on a 245 bp of the vector including siRNA backbone sequences to confirm integration of siRNAs. Primer sequences are listed in table 2. The following PCR program was used: 94 °C for 5 min followed by 35 cycles of 94 °C for 1 min, 59 °C for 45s, 72 °C for 1 min, and 72 °C for 10 min. Primer sequences are listed in **Table 3-1**.

Quantitative real-time PCR analysis for absolute quantification of transgene copy number

Absolute quantification using quantitative real-time PCR (qPCR) was performed to determine transgene copy number in transformed plants. Total reaction volume for each sample was 10 µl

containing 60 ng of genomic DNA, 30 pmol of forward and reverse primers, and 7.3 µl of iQtm SYBR® Green Supermix (Bio-Rad). Forward and reverse primers designed within the T-DNA region amplifying osa-MI-528 backbone were used as markers (**Table 3-1**). GAPDH which has one copy number in tomato was used as the reference gene to determine transgene copy number. The following thermal cycle was performed using CFX96 Bio-Rad thermal cycler (Bio-Rad Laboratories, Inc): 94 °C for 10 min followed by 34 cycles of 95 °C for 30 s, 58 °C for 20 s and 72 °C for 30 s. Two technical replications were used. A series of five-fold dilutions of genomic DNA plotted against Ct values to generate a standard curve. Ct values of samples and slope and intercept of standard curve were used to calculate transgene copy number using the following formula: $Ct_{(samples)} = slope_{(standard.curve)} \times \log_{(copy.number)} + intercept_{(standard.curve)}$ formula (Edros et al., 2013).

RNA isolation, semi-quantitative RT-PCR and end-point PCR analysis

Transgenic plants confirmed by PCR were further subjected to semi-quantitative reverse transcription (RT)-PCR to check whether integrated T-DNA is successfully transcribed in lettuce. Total RNA was isolated using the TRIzol reagent (Invitrogen, Carlsbad, CA), and was treated with RNase free DNase I to eliminate genomic DNA contamination. One µg of RNA was used for cDNA synthesized using oligo(dT) primer following the manufacturer's instructions (Revert Aid First Strand cDNA Synthesis kit, ThermoFisher, Waltham, MA, USA). The semi-quantitative RT-PCR was carried out by using a specific set of primers designed to amplify 245 bp containing primary amiRNA sequence from the expression cassette. The following thermocycler program was used to detect our target: 94 °C for 5 min followed by 35 cycles of 94 °C for 1 min, 59 °C for 45s, 72 °C for 1 min, and 72 °C for 10 min.

Next, we tested whether primary amiRNA generates mature amiRNA. Due to the short length of mature amiRNA, their detection using standard PCR was not possible. To detect mature

amiRNA in transgenic plants, a set of stem-loop primers was used in the reverse transcriptase process to add a 50 bp molecule to mature amiRNAs. cDNA was synthesized using stem-loop RT primer with the complement of 6 nucleotides from 3' end of mature amiRNA. Reverse transcription was performed in the following sequential incubation: 40 cycles of 95 °C, 85 °C, 75 °C, 65 °C, 55 °C, 45 °C, 35 °C, 25 °C, 15 °C for 15 s each to ensure proper formation of hairpin structure and annealing of reverse transcription primers, followed by 42 °C for 5 min and 75 °C for 10 min. To design forward primer, the first 12-14 nucleotides from 5' end of mature amiRNAs were selected, then an additional 6-7 5' nucleotides were added to achieve a T_m of 60 °C. A universal reverse primer within the stem-loop was used (Hou et al., 2017). The following end-point PCR program was run for amiRNA amplification: 94 °C for 2 min followed by 40 cycles of 94 °C for 15 s and 57 °C for 30 s.

Quantitative real-time PCR analysis

qPCR, the analysis was carried out to quantify relative expression levels of mature C3 and CF7 amiRNAs. cDNA was synthesized as described at the end-point PCR section with the difference of adding oligo(dT)₁₈ primer as well as amiRNAs' specific primers, to be able to reverse transcribe housekeeping gene along with target amiRNAs. Tonoplast intrinsic protein 41 (TIP-41) was used as a control to normalize Ct values. For each transgenic line RNA was isolated from 0.35 g of lettuce leaf and yielded ~20-50 µg of total RNA for different lines. Two µg of total RNA was used to synthesis cDNA. Each reaction contained 8 µl of cDNA (1:6 dilution), 0.35 µl of each forward and reverse primer (10 mM) (**Table 3-1**), and 11.3 µl of iQ_{tm} SYBR® Green Supermix in a total volume of 20 µl. qPCR was performed in two technical replications by using CFX96 Bio-Rad thermal cycler with the following program: 95 °C for 3 min, followed by 39 cycles of 95 °C

for 30 s, 55 °C for 20 and 72 °C for 30 s. Ct values were analyzed using the $2^{-\Delta C_t}$ method (Livak and Schmittgen, 2001).

RESULTS

Construction of siRNA expression vectors

In this study, lettuce was used to produce dietary amiRNAs designed to target C3 and CF7 mRNAs, respectively. An endogenous rice miRNA backbone, a 245 bp fragment of *osa-MIR528*, was customized to design amiRNAs targeting C3 and CF7 proteins of a mouse (Warthmann et al., 2008; Yan et al., 2012). C3 and CF7 amiRNA sequences were manually designed with annotation of mouse genome sequences, and the 21 bp of *osa-MIR528* was replaced by C3 and CF7 amiRNA sequences using PCR, respectively. NPTII gene enabled the selection of transgenic plants on kanamycin media and through plant DNA analysis using PCR. DNA from all transgenic lines showed the 750 bp band corresponding to the NPTII marker size. No PCR product was detected for control plants (**Figure 3-2a**).

Analysis of transgenic plants by PCR

We have generated each of three independent C3 (*C3siRNA-1*, -2, and -3) and CF7 (*CF7siRNA-1*, -2, and -3) transgenic lines, self-pollinated, and the progeny lines were genotyped for the presence of T-DNA. 245 bp of the vector including amiRNA sequences were used as a size control marker to confirm the insertion of amiRNA sequences into genomic DNA. DNA from all transgenic lines showed the 245 bp band corresponding to the marker size. No PCR product was detected for control plants (**Figure 3-2b**). The 3-month-old *C3*- and *CF7siRNA*-expressing lettuce plants were comparable to wild-type plants, and the phenotype and yield of the *C3*- and *CF7siRNA*-expressing lettuce plants were indistinguishable from the wild-type plants grown under normal growth conditions (**Figure 3-2c**). The expression of C3 and CF7 siRNAs does not appear to have any adverse effects on overall plant morphology. Transgene copy number analysis also confirmed

the successful integration of two to six copies of T-DNA within the genome of transgenic lettuce lines (**Figure 3-3a &b**).

Detection of primary and mature siRNAs

PCR confirmed transgenic plants were subjected to semi-quantitative RT-PCR. Semi-quantitative RT-PCR results showed 245 pb bands according to the expected size of primary siRNAs. However, control plants did not show any band (**Figure 3-4a**).

Next, we tested whether primary siRNAs generate mature siRNAs. Due to the short length of mature siRNAs which is almost the same size as a PCR primer, the detection of mature siRNAs using standard PCR is not possible. To amplify a molecule its length must be at least twice of a PCR primer, hence, to detect mature siRNA stem-loop primers were used in reverse transcriptase process to add a 50 bp molecule to mature siRNAs and make their amplification possible (Varkonyi-Gasic et al., 2007). End-point PCR results using specific forward and universal reverse primers in transgenic plants showed a band with the expected size of 55 bp while no band was observed in control plants (**Figure 3-4b**). To further validate our results, end-point PCR products containing mature amiRNAs were sequenced and analyzed. Sequencing data also confirmed the generation of mature amiRNAs (**Figure 3-4c &d**). These results indicate that the primary hairpin amiRNAs were produced and then cleaved to functional siRNAs.

Relative expression levels of mature amiRNAs

Transgenic lines with the lowest expression level (the highest Ct value), were selected as a control to calculate relative expression levels of amiRNAs for each transgenic line and compare their fold change expression. Data analysis showed *C3siRNA-2*-expressing lettuce had the highest expression level compared to *C3siRNA-1* and 3 lines, and *CF7siRNA-2*-expressing lettuce had the highest expression level compared to *CF7siRNA-1* and 3. Relatively low Ct values of

amiRNAs compared with reference gene showed mature amiRNAs are expressed in detectable levels and higher than a housekeeping gene such as TIP-41 suggesting the high possibility of adequate production for later feeding experiments (**Figure 3-5**).

DISCUSSION

Since the emergence of RNAi technology, many papers have been published on therapeutic potentials of siRNAs, reporting diet-based siRNAs can successfully reduce expression levels of target mRNAs in animal and human cells. Chin et al., detected plant miR159 in human sera and showed its effects on inhibition of breast cancer (Chin et al., 2016). In *Bactericera cockerelli* oral feeding of siRNAs decreased targeted mRNA levels (Wuriyangan et al., 2011). To utilize this technology several studies have been conducted to find the best feeding diet in animals to improve siRNA uptake through digestive system. A honeysuckle diet in mice enhanced the detection of MIR2911 and MIR168a (Yang et al., 2015). Plant miRNA was also detected in human plasma through watermelon feeding (Liang et al., 2015). In the present study, we have expressed and detected primary amiRNAs targeting mouse mRNAs in lettuce tissues using RT-PCR. We subsequently, validated proper cleavage of primary amiRNAs by Dicer and generation of mature single-stranded amiRNAs by stem-loop end-point PCR, qRT-PCR, and Sanger sequencing. Primary miRNAs present in raw plant tissues and DNA fragments are not available in cooked plant tissues. Also, plant primary miRNAs cannot survive through animal or human's digestive system. However, mature plant miRNAs are detected in both cooked foods and human blood and tissues (Zhang et al., 2012). Thus, these siRNA expressing lettuce lines, that not only can produce primary amiRNAs, but also can generate mature amiRNAs, have great potentials for the successful delivery of mature CF7 and C3 siRNAs into animal cells to target blood clotting factors in therapeutic trials. The expression vector system established here can be utilized to produce any animal siRNAs in lettuce or other dicot plants for further therapeutic purposes.

REFERENCES

- Aagaard, L., Rossi, J. J. (2007). RNAi therapeutics: principles, prospects, and challenges. *Advanced drug delivery reviews*, 59, 75-86.
- Beckman, M.G., Hooper, W.C., Critchley, S.E. and Ortel, T.L. (2010). Venous thromboembolism: a public health concern. *American journal of preventive medicine*, 38(4), S495-S501.
- Bobbin, M.L. & Rossi, J.J. (2016). RNA interference (RNAi)-based therapeutics: delivering on the promise? *Annual review of pharmacology and toxicology*, 56, 103-122.
- Chen, C., Ridzon, D. A., Broomer, A. J, Zhou, Z., Lee, D. H., Nguyen, J. T., Barbisin, M., Xu, N. L., Mahuvakar, V. R., Andersen, M. R., Lao, K. Q., Livak, K. J., Guegler, K. J. (2005). Real-time quantification of microRNAs by stem-loop RT-PCR. *Nucleic Acids Res*, 20, e179.
- Chin, A. R., Fong, M. Y., Somlo, G., Wu, J., Swiderski, P., Wu, X., Wang, S. E. (2016). Cross-kingdom inhibition of breast cancer growth by plant miR159. *Cell research*, 26, 217-228.
- Cho, W. C. (2010). MicroRNAs: potential biomarkers for cancer diagnosis, prognosis and targets for therapy. *The international journal of biochemistry & cell biology*, 42, 1273-81.
- David, B. (2004). RNA silencing in plants. *Nature*, 431, 356-363.
- Davoodi Mastakani, F., Pagheh, G., Rashidi Monfared, S., Shams-Bakhsh, M. (2018). Identification and expression analysis of a microRNA cluster derived from pre-ribosomal RNA in *Papaver somniferum* L. and *Papaver bracteatum* L. *PLoS ONE*, 13, e0199673.

- DiScipio, R.G., Chakravarti, D.N., Muller-Eberhard, H.J. & Fey, G.H. (1988). The structure of human complement component C7 and the C5b-7 complex. *Journal of Biological Chemistry*, 263(1), 549-560.
- Edros, R.Z., McDonnell, S. & Al-Rubeai, M. (2013). Using molecular markers to characterize productivity in Chinese hamster ovary cell lines. *PLoS One*, 8(10), e75935.
- Fischer, R., Stoger, E., Schillberg, S., Christou, P., Twyman, R. M. (2004). Plant-based production of biopharmaceuticals. *Curr Opin Plant Biol*, 7, 152-158.
- Higuchi, Y., Kawakami, S., Hashida, M. (2010). Strategies for In Vivo Delivery of siRNAs. *BioDrugs*, 24, 195.
- Hou, Y.H., Jeyaraj, A., Zhang, X. & Wei, C.L., (2017). Absolute quantification of microRNAs in green tea (*Camellia sinensis*) by stem-loop quantitative real-time PCR. *Journal of the Science of Food and Agriculture*, 97(9), 2975-2981.
- Hu, S., Huang, M., Li, Z., Jia, F., Ghosh, Z., Lijkwan, M. A., Fasanaro, P., Sun, N., Wang, X., Martelli, F., Robbins, R. C. (2010). MicroRNA-210 as a novel therapy for treatment of ischemic heart disease. *Circulation*, 122, S124-31.
- Janssen, B.J., Huizinga, E.G., Raaijmakers, H.C., Roos, A., Daha, M.R., Nilsson-Ekdahl, K., Nilsson, B. & Gros, P. (2005). Structures of complement component C3 provide insights into the function and evolution of immunity. *Nature*, 437(7058), 505-511.

- Kanamoto, H., Yamashita, A., Asao, H., Okumura, S., Takase, H., Hattori, M., Yokota, A., Tomizawa, K. I. (2006). Efficient and stable transformation of *Lactuca sativa* L. cv. Cisco (lettuce) plastids. *Transgenic research*, 15, 205-17.
- Kedmi, R., Veiga, N., Ramishetti, S., Goldsmith, M., Rosenblum, D., Dammes, N., Hazan-Halevy, I., Nahary, L., Leviatan-Ben-Arye, S., Harlev, M. & Behlke, M. (2018). A modular platform for targeted RNAi therapeutics. *Nature nanotechnology*, 13(3), 214-219.
- Kota, J., Chivukula, R. R., O'Donnell, K. A., Wentzel, E. A., Montgomery, C. L., Hwang, H. W., Chang, T. C., Vivekanandan, P., Torbenson, M., Clark, K. R., Mendell, J. R. (2009). Therapeutic microRNA delivery suppresses tumorigenesis in a murine liver cancer model. *Cell*, 137,1005-17.
- Kramer, M. F. (2011). Stem-loop RT-qPCR for miRNAs. *Current protocols in molecular biology*, Chapter 15, Unit 15.10.
- Lares, M. R., Rossi, J. J., Ouellet, D. L. (2010). RNAi and small interfering RNAs in human disease therapeutic applications. *Trends in biotechnology*, 28, 570-579.
- Liang, H., Zhang, S., Fu, Z., Wang, Y., Wang, N., Liu, Y., Zhao, C., Wu, J., Hu, Y., Zhang, J., Chen, X. (2015). Effective detection and quantification of dietetically absorbed plant microRNAs in human plasma. *The Journal of nutritional biochemistry*, 26, 505-12.
- Livak, K.J. & Schmittgen, T.D., (2001). Analysis of relative gene expression data using real-time quantitative PCR and the 2- $\Delta\Delta$ CT method. *methods*, 25(4), 402-408.
- M Simon- US Patent 4,425,908, 1984 - Google Patents.

- Murashige, T., Skoog, F. (1962). A Revised Medium for Rapid Growth and Bio Assays with Tobacco Tissue Cultures. *Physiologia Plantarum*, 15, 473-497.
- Park, S., Elless, M. P., Park, J., Jenkins, A., Lim, W., Chambers, I. E., Hirschi, K. D. (2009). Sensory analysis of calcium-biofortified lettuce. *Plant Biotechnology Journal*, 7, 106-17.
- Petrick, J. S., Brower-Toland, B., Jackson, A. L., Kier, L. D. (2013). Safety assessment of food and feed from biotechnology-derived crops employing RNA-mediated gene regulation to achieve desired traits: a scientific review. *Regulatory Toxicology and Pharmacology*, 66, 167-76.
- Petrovska, B. B. (2012). Historical review of medicinal plants' usage. *Pharmacognosy reviews*, 6, 1-5.
- Rivard, G. E., Brummel-Ziedins, K. E., Mann, K. G., Fan, L., Hofer, A., Cohen, E. (2005). Evaluation of the profile of thrombin generation during the process of whole blood clotting as assessed by thrombelastography. *Journal of Thrombosis and Haemostasis*, 3, 2039-43.
- Schillberg, S., Zimmermann, S., Voss, A., Fischer, R. (1999). Apoplastic and cytosolic expression of full-size antibodies and antibody fragments in *Nicotiana tabacum*. *Transgenic research*, 8, 255-63.
- Sioud, M. (2004). Therapeutic siRNAs. *Trends in pharmacological sciences*, 25, 22-28.
- Tatiparti, K., Sau, S., Kashaw, S. K., Iyer, A. K. (2017). siRNA Delivery Strategies: A Comprehensive Review of Recent Developments. *Nanomaterials*, 7, 77.

- Varkonyi-Gasic, E., Wu, R., Wood, M., Walton, E. F., Hellens, R. P. (2007). Protocol: a highly sensitive RT-PCR method for detection and quantification of microRNAs. *Plant methods*, 3, 1-2.
- Voinnet, O., Pinto, Y.M. & Baulcombe, D.C. (1999). Suppression of gene silencing: a general strategy used by diverse DNA and RNA viruses of plants. *Proceedings of the National Academy of Sciences*, 96(24), 14147-14152.
- Wang, K., Li, H., Yuan, Y., Etheridge, A., Zhou, Y., Huang, D., Wilmes, P., Galas, D. (2012). The complex exogenous RNA spectra in human plasma: an interface with human gut biota? *PloS one*, 7, e51009.
- Warthmann, N., Chen, H., Ossowski, S., Weigel, D., Hervé, P. (2008). Highly specific gene silencing by artificial miRNAs in rice. *PLoS One*, 3, e1829.
- Wuriyangan, H., Rosa, C., Falk, B. W. (2011). Oral delivery of double-stranded RNAs and siRNAs induces RNAi effects in the potato/tomato psyllid, *Bactericerca cockerelli*. *PLoS One*, 6, e27736.
- Yan, F., Lu, Y., Wu, G., Peng, J., Zheng, H., Lin, L. & Chen, J. (2012). A simplified method for constructing artificial microRNAs based on the osa-MIR528 precursor. *Journal of biotechnology*, 160(3-4), 146-150.
- Yang, Elbaz-Younes I., Primo, C., Murungi, D., Hirschi, K. D. (2018). Intestinal permeability, digestive stability and oral bioavailability of dietary small RNAs. *Scientific reports*, 8, p.10253.

Yang, J., Farmer, L. M., Agyekum, A. A., Hirschi, K. D. (2015). Detection of dietary plant-based small RNAs in animals. *Cell research*, 25, 517-20.

Yang, J., Hotz, T., Broadnax, L., Yarmarkovich, M., Elbaz-Younes, I., Hirschi, K. D. (2016). Anomalous uptake and circulatory characteristics of the plant-based small RNA MIR2911. *Scientific reports*, 6, 26834.

Zhang, L., Hou, D., Chen, X., Li, D., Zhu, L., Zhang, Y., Li, J., Bian, Z., Liang, X., Cai, X., Yin, Y. (2012). Exogenous plant MIR168a specifically targets mammalian LDLRAP1: evidence of cross-kingdom regulation by microRNA. *Cell research*, 22, 107-26.

FIGURES

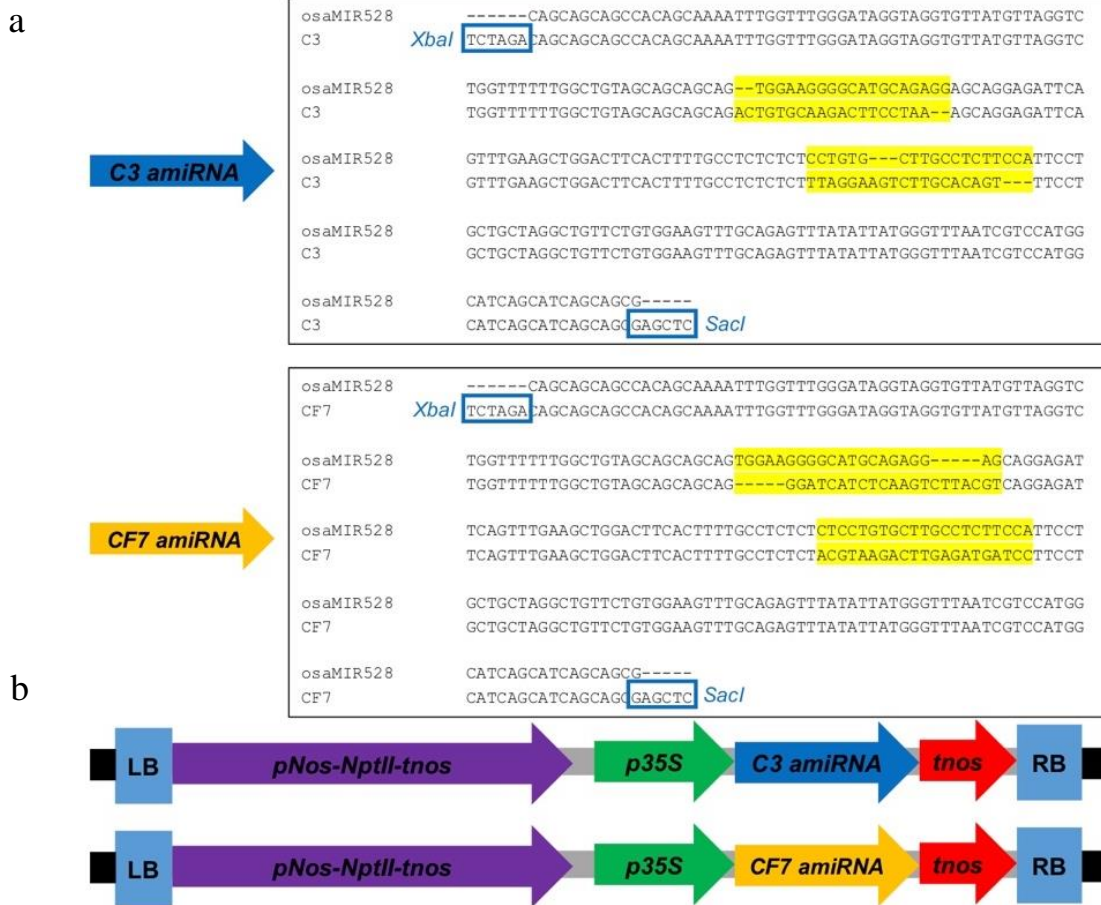


Figure 3-1 Plant expression vectors harboring amiRNAs designed to target C3 and CF7 messenger RNAs of mouse using a 245-bp fragment of osa-MIR528.

(a) The 21 bp of osa-MIR528 (black letters) from the stem-loop sequence was replaced by C3 (top panel) and CF7 (bottom panel) sequences (red letters) to create siRNAs, respectively. The cloning sites used were *Xba*I and *Sac*I which insert a fragment of approximately 259 bp after restriction digestion. (b) Map of T-DNA region of the binary vectors (top panel, *pC3amiRNA*; bottom panel, *pCF7amiRNA*) used for transformation.

LB: Left border; NPTII: Neomycin phosphotransferase; p35S: Cauliflower mosaic virus 35S promoter; pNos: Nopaline synthase promoter; RB: Right border; tnos: Nopaline synthase terminator.

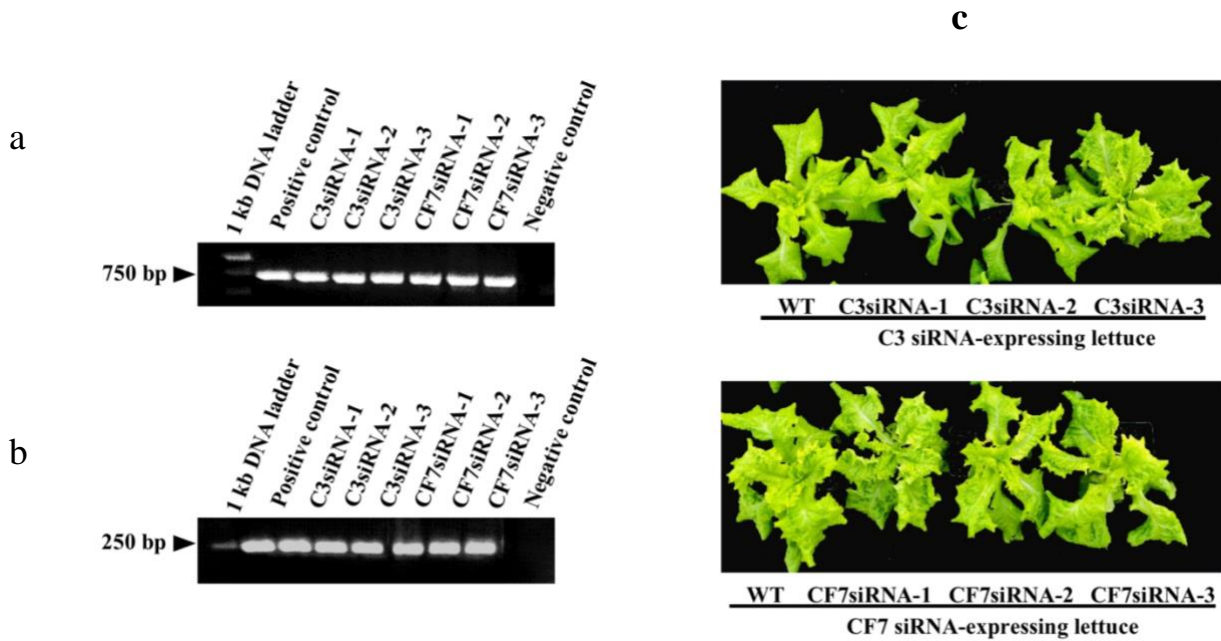
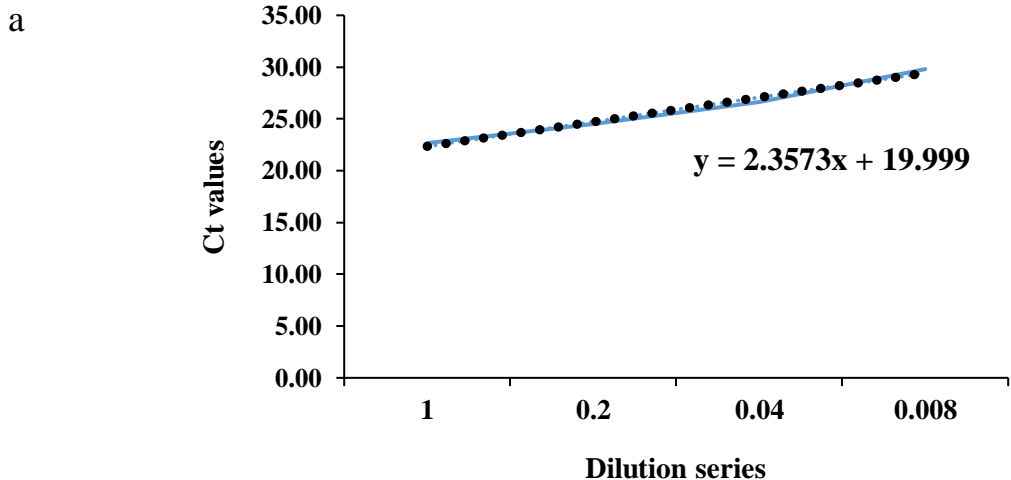


Figure 3-2 Molecular and phenotype analyses of C3siRNA- and CF7siRNA-expressing lettuces.

(a) PCR detection of *NPTII* gene in the genomic level of transformed lettuce plants. (b) PCR detection of C3 and CF7 artificial microRNA inserts in lettuce genomic DNA. Positive control, artificial microRNAs; negative control, wild-type lettuce. Primer sequences are shown in Table 1. (c) Phenotypes of *C3siRNA*-expressing, *CF7siRNA*-expressing, and WT lettuce plants. *NPTII*: Neomycin phosphotransferase II gene; WT: Wild-type.



b

Line	Ct value	Slope	Intercept	Copy number
C3siRNA-1	22.82075835	2.3573	19.999	3
C3siRNA-2	23.46711329	2.3573	19.999	4
C3siRNA-3	23.07162938	2.3573	19.999	4
CF7siRNA-1	22.18402437	2.3573	19.999	3
CF7siRNA-2	24.34534104	2.3573	19.999	6
CF7siRNA-3	21.9701288	2.3573	19.999	2

Figure 3-3 Absolute quantification of transgene copy number in C3siRNA- and CF7siRNA-expressing lettuces using quantitative real-time PCR.

(a) Standard curve showing Ct values plotted against a series of 5-fold DNA dilutions. (b) Transgene copy number results using a standard curve for primary C3 and CF-7 artificial microRNA backbones. Data were analyzed using the following formula:

$$Ct(\text{samples}) = \text{slope}(\text{standard.curve}) \times \log(\text{copy.number}) + \text{intercept}(\text{standard.curve}).$$

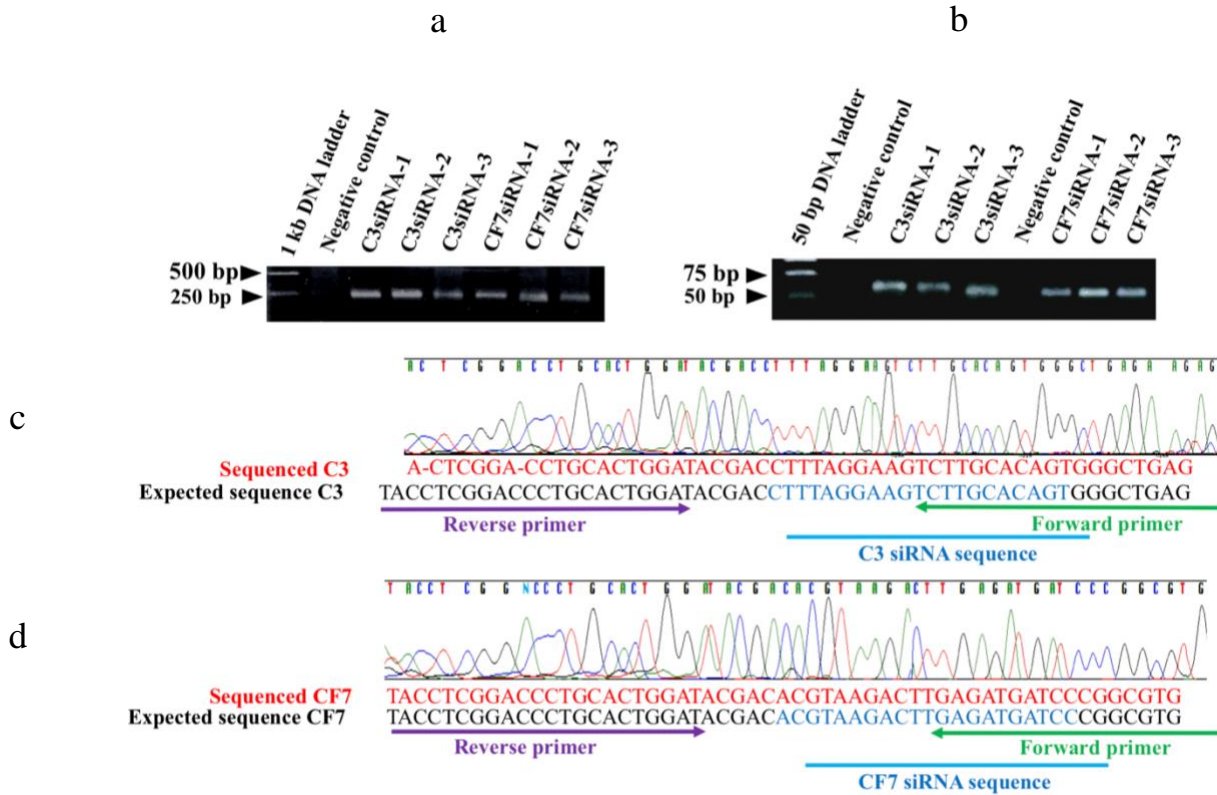


Figure 3-4 PCR detection of primary and mature amiRNAs and Sanger sequencing of mature C3 and CF7 amiRNAs using stem-loop universal reverse primer.

(a) RT-PCR detection of primary C3 and CF7 amiRNAs from *C3siRNA*- and *CF7siRNA*-expressing lettuces. Negative control, wild-type lettuce. (b) Stem-loop endpoint PCR detection of mature C3 and CF7 amiRNAs from *C3siRNA*- and *CF7siRNA*-expressing lettuces. Negative control, wild-type lettuce. Primer sequences are shown in Table 3-1. (c) Expected and obtained sequences of mature C3 amiRNA. (d) Expected and obtained sequences of mature CF7 amiRNA.

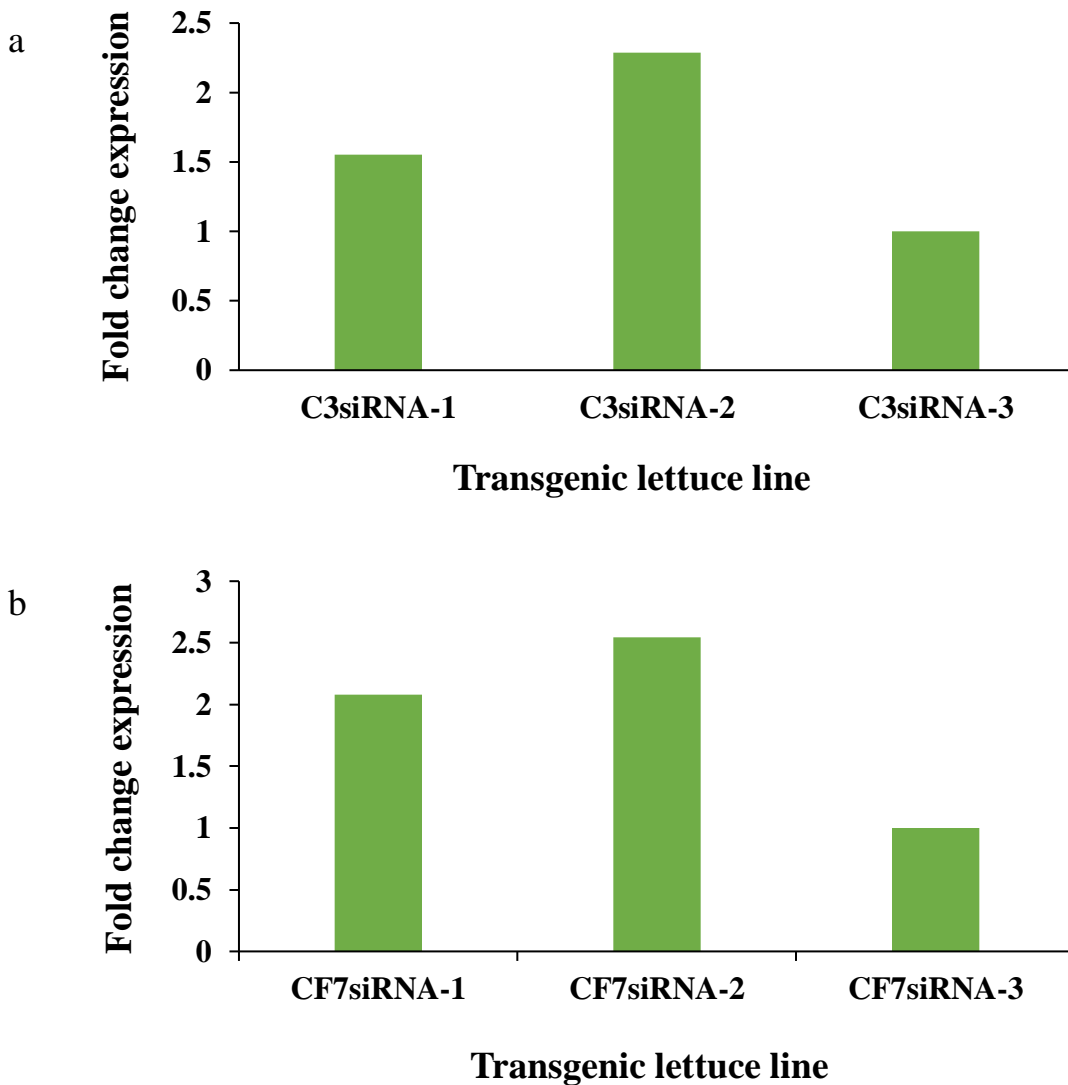
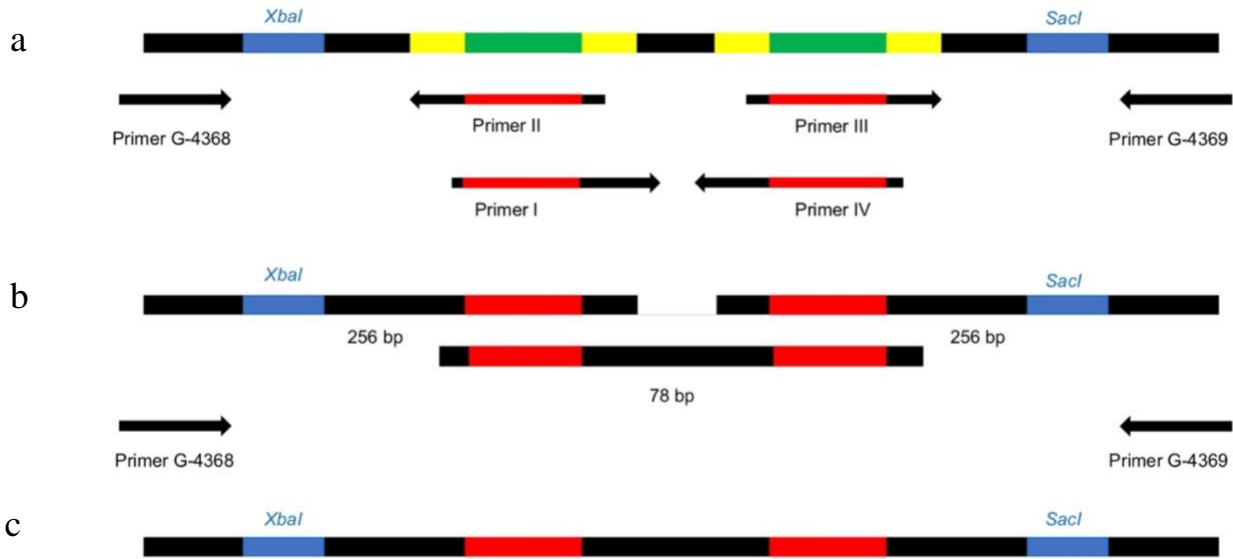


Figure 3-5 Quantitative real-time PCR analysis of mature C3 and CF7 artificial microRNAs (amiRNAs) in *C3siRNA*- and *CF7siRNA*-expressing lettuces using stem-loop primer.

(a) Fold change expression of mature C3 amiRNA in different transgenic lines compared to line with the lowest expression level of C3 amiRNA. (b) Fold change expression of mature CF7 amiRNA in different transgenic lines compared to line with the lowest expression level of CF7 amiRNA. *TIP-41* (Tonoplastic intrinsic protein 41) was used as internal control and data were analyzed by Livak method. Primer sequences are shown in Table 3-1.



Supplementary Figure S 3-1 PCR scheme to produce artificial microRNA construct.

(a) The original rice micro RNA 528 sequences (green) were replaced by C3 and CF7 artificial microRNA sequences (red) during the first PCR using three pairs of primers. Primer sequences are shown in Supplementary Table S3-1. Yellow sequences are complementary to primers and multiple cloning sites are shown in blue. (b) Three DNA fragments were amplified during PCRs and were combined by fusion PCR using G-4368 and G-4369 primers to obtain one DNA sequence. (c) Final DNA sequence ready for subsequent cloning.

TABLES

Table 3-1 Primer sequences.

Experiment		Forward primer	Reverse primer
NPTII PCR		5'-gaggctattcggctatgactg-3'	5'-atcgggagcggcgataaccgta-3'
Primary amiRNA detection, PCR & Transgene copy number detection, quantitative real-time PCR		5'-cagcagcagccacagcaaaat-3'	5'-atggcatcagcatcagcagc-3'
Primary amiRNA detection, reverse transcriptase PCR		5'-cagcagcagccacagcaaaat-3'	5'-atggcatcagcatcagcagc-3'
Quantitative real-time PCR, internal control gene (tonoplast intrinsic protein 41)		5'-gagagatttgctggagggaacta-3'	5'-ccttgactgatgatggttga-3'
Mature amiRNA detection, end-point PCR & Mature miRNA quantification, quantitative real-time PCR	Complement 3	5'-ctcagcccactgtgcaagac-3'	5'-ccagtgcagggtccgagga-3'
	Coagulation factor 7	5'-cacgccgggatcatctcaa-3'	5'-ccagtgcagggtccgagga-3'
Stem-loop reverse transcriptase	Complement 3	5'-gtcgtatccagtgcagggtccgaggtattcgactggatacagaccttag-3'	
	Coagulation factor 7	5'-gtcgtatccagtgcagggtccgaggtattcgactggatacagaccttag-3'	

Supplementary Table 3-1

Primer name	Primer sequence
G-4368-F	5'-ctgcaaggcgattaagttgggtaac-3'
G-4369-R	5'-gcfgataacaatttcacacaggaaacag-3'
Complement 3, forward I	5'-agactgtgcaagacttcctaaagcaggagattcagttga-3'
Complement 3, reverse II	5'-tgcttaggaagtcttgacagtctgctgctgtacagcc-3'
Complement 3, forward III	5'-ctcttaggaagtcttgacagtttctgctgctaggctg-3'
Complement 3, reverse III	5'-aaactgtgcaagacttcctaaagagagaggcaaaagtgaa-3'
Coagulation Factor 7, forward I	5'-agggatcatctcaagtcttacgtcaggagattcagttga-3'
Coagulation Factor 7, reverse II	5'-gacgtaagacttgagatgatccctgctgctgtacagcc-3'
Coagulation Factor 7, forward III	5'-ctacgtaagacttgagatgatccttctgctgctaggctg-3'
Coagulation Factor 7, reverse III	5'-aaggatcatctcaagtcttacgtagagaggcaaaagtgaa-3'